IOWA STATE UNIVERSITY
Digital Repository

Graduate Theses and Dissertations

Iowa State University Capstones, Theses and Dissertations

2015

Parametric modeling for simulation based hypersonic vehicle design

Alexander David Lee
Iowa State University

Follow this and additional works at: https://lib.dr.iastate.edu/etd

Part of the Aerospace Engineering Commons

Recommended Citation
Lee, Alexander David, "Parametric modeling for simulation based hypersonic vehicle design" (2015). *Graduate Theses and Dissertations*. 14398.
https://lib.dr.iastate.edu/etd/14398

This Thesis is brought to you for free and open access by the Iowa State University Capstones, Theses and Dissertations at Iowa State University Digital Repository. It has been accepted for inclusion in Graduate Theses and Dissertations by an authorized administrator of Iowa State University Digital Repository. For more information, please contact digirep@iastate.edu.

Parametric modeling for simulation based hypersonic vehicle design

by

Alexander David Lee

A thesis submitted to the graduate faculty
in partial fulfillment of the requirements for the degree of

MASTER OF SCIENCE

Major: Aerospace Engineering

Program of Study Committee
Thomas P. Gielda, Co-Major Professor
Richard W. Wlezien, Co-Major Professor
Thomas Ward III

Iowa State University

Ames, Iowa

2015

Copyright © Alexander David Lee, 2015. All rights reserved.

TABLE OF CONTENTS

Page

LIST OF FIGURES iv
LIST OF TABLES vi
NOMENCLATURE vii
ACKNOWLEDGEMENTS ix
ABSTRACT x
CHAPTER 1. INTRODUCTION 1
1.1 General Proceedings 3
CHAPTER 2. BACKGROUND 4
2.1 Motivation 4
2.2 Design Methods 5
2.2.1 Historical 5
2.2.2 Brief History of Computer Aided Engineering 5
2.3 Top Down Design Methodology 8
2.3.1 Requirements 8
2.3.2 Conceptual Concurrent Design 10
2.3.3 Preliminary Concurrent Design 12
2.3.4 Detailed Design 12
CHAPTER 3. INTELLEGENT CAD MODELS 14
3.1 Initial Sizing and Design 15
3.2 Construction Methodology Overview 15
3.2.1 CAD Tool Definitions 15
3.2.2 Simple Parametric Example 19
3.3 iMod Construction Process 22
3.4 Blended Wing-Body Aircraft: Hypersonic Wave Rider 22
3.4.1 Design Parameters 22
3.4.2 Construction Process 24
3.5 Traditional Wing-Body Aircraft: Supersonic Transport 37
3.5.1 Design Parameters 37
3.5.2 Summary of Construction Process 40
CHAPTER 4. SIMULATION BASED DESIGN METHODOLOGY 42
4.1 Physics Simulation Setup (CFD) 43

4.1.1 Geometry 43
4.1.2 Physics Continua 44
4.1.3 Mesh Continua 45
4.1.4 Boundary Conditions 46
4.1.5 Force and Moment Reports 47
4.2 Performance Evaluations 48
4.2.1 L/D 48
4.2.2 Static Stability 49
4.2.3 Total Volume 51
4.2.4 Scoring Performance Metrics 51
4.3 Design Changes 52
4.3.1 Trade Studies 52
4.3.2 Optimization Schema 52

CHAPTER 5. CASE STUDY 53
5.1 Requirements 53
5.2 Design Targets 53
5.3 Initial Concept Model 53
5.4 iMod 54
5.5 Physics Simulations 56
5.6 Performance Evaluations 57
5.6.1 L/D + Breguet Range Equation 58
5.6.2 Volume + Modified Breguet Range Equation 59
5.6.3 Range from Energy-State Approximation 61
5.6.4 Static Stability 65
5.6.5 Lift 66

CHAPTER 6. CONCLUSION 67
6.1 Future Work 68

BIBLIOGRAPHY 69

LIST OF FIGURES

Page
Figure 1.1: Design changes and their impact on project cost for design phases. 1
Figure 1.2: Section view of surface gaps in Busemann inlet geometry. 2
Figure 2.1: National Aerospace Plane. 6
Figure 2.2: Ford Motor Company UPV simulation in a wind tunnel [6]. 6
Figure 2.3: Interior cabin thermal comfort model (left) and simulation (right) [6]. 7
Figure 2.4: Refrigeration systems incorporated into Whirlpools SBD process [7]. 8
Figure 2.5: Simplified QFD chart and legend. 9
Figure 2.6: Conceptual design flow chart. 10
Figure 2.7: Sample diagram for a CAD-centric design environment. 11
Figure 2.8: Example of a conceptual design scorecard for multiple vehicle variations. 12
Figure 3.1: Intelligent relation between inlet capture area and outer nacelle diameter. 14
Figure 3.2: Parent-child relationships. Original sketch positions. 18
Figure 3.3: Parent-child relationships. "Centerline" sketch alteration. 18
Figure 3.4: Parent-child relationships. "Height Control" sketch alteration. 19
Figure 3.5: Simple example of iMod parametric control sketches. 20
Figure 3.6: iMod with body cross section sketches and guide curves included. 21
Figure 3.7: Simple loft variations between two rectangular cross sections. 21
Figure 3.8: Design approach to ramjet/scramjet inlets at design Mach number. 23
Figure 3.9: Mid-plane high and low pressure contours. 23
Figure 3.10: Reference coordinate system. 24
Figure 3.11: Centerline body section angles. Detail view of nose LE thickness control. 25
Figure 3.12: Body thickness control reference sketch (cyan) and centerline sketch (black). 26
Figure 3.13: Lateral control sketches. Span and dihedral (black). Thickness (magenta). ... 27
Figure 3.14: Lateral control sketches. Span and dihedral (black). Thickness (magenta). ... 28
Figure 3.15: Display of all lateral and longitudinal control sketches. 28
Figure 3.16: Progression through construction stages of a feature sketch. 29
Figure 3.17: Tangency magnitude control comparison for body feature splines. 30
Figure 3.18: Model display state after all body feature sketches added. 31
Figure 3.19: Vertical stabilizer planform reference sketches (cyan) and planes. 32
Figure 3.20: Final reference sketch display state for vertical stabilizer. 32

Figure 3.21: Loft without guide curves (top) and with guides (bottom). 33
Figure 3.22: Mirror plane and wing leading edge guide curves. 34
Figure 3.23: Web of point-to-point guide curves..... 35
Figure 3.24: SolidWorks CAD environment for lofting between sketch profiles. 36
Figure 3.25: Final configuration display state (left). Robustness test (right). 36
Figure 3.26: Wing dihedral set to 5° (left). Wing anhedral set to 5° (right)..... 37
Figure 3.27: Wing span variations. b=83’ 4” (left) and b=114’ 7” (right). 38
Figure 3.28: Wing t/c ratio variations. 38
Figure 3.29: Wing sweep variations. 39
Figure 3.30: Vertical stabilizers. Single (left) and dove tail (right) configurations..... 39
Figure 3.31: Control surface deflections..... 40
Figure 4.1: Simulation based design process flow chart..... 42
Figure 4.2: Profile used for free stream air domain. 44
Figure 4.3: Initial geometry and remeshed surface comparison. 45
Figure 4.4. Half (left) and full (right) body simulation boundary conditions..... 47
Figure 4.5: Standard body fixed stability coordinate system..... 48
Figure 5.1: Initial hypersonic wave rider concept model. 54
Figure 5.2: Example of a design table (segment from batches 1, 2, and 3)..... 55
Figure 5.3: Naming conventions from iMod. 56
Figure 5.4: Individual lift to drag ratios for 56 variations. 58
Figure 5.5: Breguet range evaluations relative to 5000 nm target..... 59
Figure 5.6: Volume breakdowns for each model variation..... 60
Figure 5.7: Modified Breguet range evaluations for cruise relative to the 5000 nm target... 61
Figure 5.8: Energy method trajectory results: Baseline configuration (PS01_V01). 62
Figure 5.9: Energy method trajectory results: Baseline configuration (PS01_V35). 63
Figure 5.10: Energy method trajectory results: Baseline configuration (PS01_V33). 63
Figure 5.11: Energy method trajectory results: Baseline configuration (PS01_V16). 64
Figure 5.12: Static margin values for each variation (relative to the 4.0% target)..... 66
Figure 5.13: Lift relative to 10,000 lb_f target for each variation..... 66

LIST OF TABLES

Page

Table 4.1: Abbreviations used in Eulerian transformation matrices..... 49

Table 5.1: Test parameters. 54

Table 5.2: Free stream flow conditions for variation studies..... 57

Table 6.1: Summarized timeline of this study. 67

NOMENCLATURE

BWB	Blended Wing Body
CFD	Computational Fluid Dynamics
FEA	Finite Element Analysis
CAD	Computer Aided Design
RANS	Reynolds Averaged Navier-Stokes
RFP	Request for Proposal
CAE	Computer Aided Engineering
DoD	Department of Defense
IGES	Integrated Graphics Exchange Specification
NASP	National Aerospace Plane
UPV	Unified Parametric Model
SBD	Simulation Based Design
TDD	Top Down Design
QFD	Quality Function Deployment
CDR	Conceptual Design Review
OML	Outer Mold Line
iMod	Intelligent CAD Model
L/D	Lift to Drag Ratio
LE	Leading Edge
REST	Rectangular-to-Elliptical Shape Transition
MDAO	Multidisciplinary Design Analysis and Optimization
UAS	Unmanned Aircraft Systems

AR	Aspect Ratio
t/c	Thickness to Chord Ratio
*.csv	Comma Separated Values (data file format)
TSFC	Thrust Specific Fuel Consumption
C_g and COG	Center of Gravity
np	Neutral Point
nm	Nautical Miles
GTOW	Gross Takeoff Weight
AoA	Angle of Attack
A_{ref}	Reference Area
MAC	Mean Aerodynamic Chord

ACKNOWLEDGEMENTS

I would like to thank my advisor, Dr. Thomas Gielda, for his guidance and expertise. Were it not for him, this endeavor would have been unmanageable. His time, patience, and encouragement have imparted me with qualities revered by the most respectable of engineering professionals. In addition, I thank the other members of my committee Dr. Richard Wlezien and Dr. Thomas Ward III for all their time and effort invested into my thesis work. I would also like to thank Boeing Military Aircraft for their financial support and the opportunity to help resolve real world engineering problems. It was a truly life changing experience.

I thank my colleagues and friends at Iowa State University for their advice and accompaniment. Including, but not limited to, Brad Kirkpatrick, David Sikorski, Michel Kurtz, and John Watson. Last but not least, I would like to thank my Mother and Father for encouraging my curiosity as a child and allowing me to take things apart in my attempt to understand how they function. With their support, I was free to develop an inquisitive disposition for the material world around me – ultimately leading me down the path of engineering.

ABSTRACT

The conceptual design stage offers the most opportunity for innovation and the capability to reveal costly design errors early. Integrating high fidelity design and simulation tools into the conceptual design stage enables engineers to develop design variations quickly and affordably. This work focuses primarily on the development and utilization of parametric modeling methods as they apply to a simulation based design process. It will also address the impacts to conceptual design development time. A blended wing-body (BWB) hypersonic wave rider demonstrates how state-of-the-art solid modeling techniques can be coupled to high fidelity CFD analysis codes to perform top down design. Performance trends are identified for several trade study variations which represent a single iteration through the simulation based design process. Performance metrics are based on interpretations from higher level customer, regulatory, business, and other requirements. The process of cascading these requirements down to the component level is the definition of top-down-design. This bidirectional tracing of requirements allows vehicle development to progress in a manner such that any change of the vehicle can be assessed in terms of the overarching requirements.

CHAPTER 1. INTRODUCTION

It is widely accepted that the best opportunities to achieve significant cost reductions are in the early stages of product development [1, 2]. Although this may seem intuitively obvious, many large organizations are still designing and developing products using outdated tools and methods. Off the shelf computational power provided by today's common desktop workstations allows companies and their engineer's access to numerous software packages. If implemented correctly, these packages have the potential to reduce conceptual design costs while also providing higher fidelity analyses. Figure 1.1 represents the impact of design changes in terms of cost through a typical product program, from conception to production.

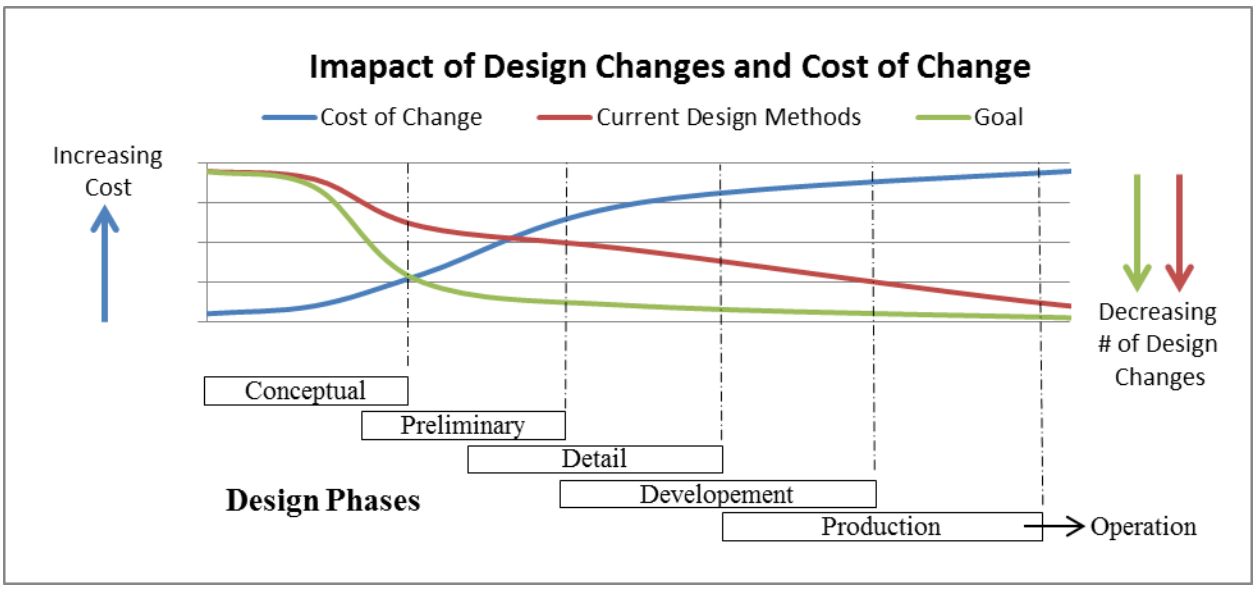

Figure 1.1: Design changes and their impact on project cost for design phases.

The figure above indicates a significant portion of design changes are generated during the conceptual design phase while capital investment is minor. This plot also elicits the impact design decisions made during conceptual design have on project costs. The more errors caught in the conceptual phase ultimately reduces costly changes later in the design process. Minimizing errors is quintessential during this first stage for project (and possibly company) success.

For the aerospace industry, the tools capable of reducing conceptual design errors are simple, commercially available computational fluid dynamic (CFD) software, finite element analysis (FEA) software, and Computer-Aided Design (CAD) software. This tool set combined with the right design process, allows for rapid almost overnight results - enabling

engineers to make informed decisions on first pass designs. The key to this design process: a robust CAD model that is common to all groups within the initial design phase. These groups may include structures, aerodynamics, and propulsion systems. This design structure will hence be referred to as CAD-centric. In addition, it is important that the CAD-centric model is intelligently parameterized and flexible. The methodology set forth in Chapter 3 defines and describes in more detail what intelligent modeling is and its role in reducing time between design iterations. The parameterized model includes features of interest to each design group built into their respective components. For example, the aerodynamics department may want control over wing sweep. By incorporating sweep as a design parameter, the CAD model may then be manipulated manually by an engineer or autonomously using an appropriate optimization routine. It is this rapid manipulation coupled with the appropriate CFD and FEA packages that give an aerodynamic engineer critical performance and loading data that a structural engineer can then map to a finite element mesh and quickly identify problematic design features early in the stages of product development.

Many aerospace companies today use surface representations (in contrast to automotive and consumer goods where they use solids) to define geometrical features needed for analysis in the conceptual and preliminary design phases. It is the intention of this paper to demonstrate an alternative method of creating robust geometries capable of rapid modifications using only solid features. Models constructed from solid bodies are ideal for CFD analysis due to their inherent manifold properties. Surface representations are difficult to analyze due in part to how they are constructed. When multiple sheets are used to create complex geometries, gaps and overlapping regions form between the adjacent sheet bodies. Figure 1.2 illustrates this complication.

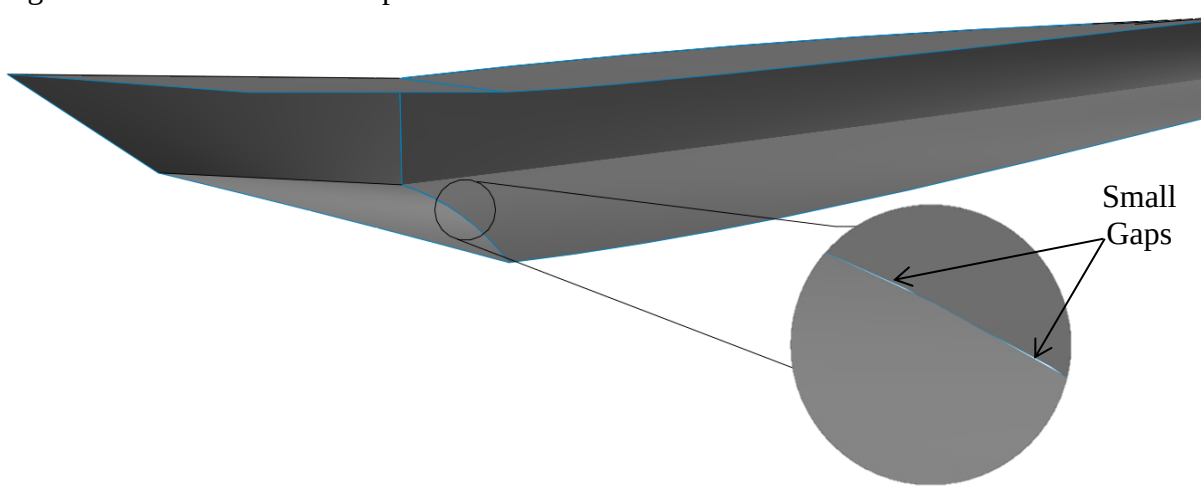

Figure 1.2: Section view of surface gaps in Busemann inlet geometry.

Gaps shown in Figure 1.2 are not evident from a distance, but as the detail view reveals, they are inherent characteristics for surface representations. These issues require many engineering man hours to correct; drastically decreasing the quantity of design variations a conceptual design team can deliver. Corrections are usually accomplished by stitching/sewing adjacent surfaces together, however, if the gaps and overlaps are not within tolerance, than other measures must be taken.

1.1 General Proceedings

This thesis will focus on parametric modeling methods as they apply to a simulation based design (SBD) process. The second chapter reviews the evolution of computer aided engineering and the historical roles it has played in industry advancements. It will also describe the proposed simulation based design process and the benefits of implementing a CAD-centric structure. Chapter three begins with an overview of what constitutes an intelligent CAD model and outlines the interrelations between aircraft design disciplines. Following that, it will detail the model construction process for an air breathing hypersonic blended wing body aircraft as well as a traditional supersonic jet configuration. Simulation methodology is characterized in chapter four. Here the simulated flight conditions, domain sizing and solvers used in STAR-CCM+ are justified, as well as the importance of using solids over surfaces. A Case study using an author designed blended wing variant encompasses chapter five. Aerodynamic efficiency, range, and static stability analyses are also calculated using MatLab to process and display data. Chapter six draws general conclusions and presents opportunities for future work.

CHAPTER 2. BACKGROUND

2.1 Motivation

Engineers inherently strive to take existing constructs and make them better. In the realm of aerodynamics, this means designing new aircraft to go faster, higher, and further than ever before. Hypersonic vehicles accomplish exactly that. With applications now extending beyond research and into space and military, the practicalities for developing fast and accurate design methods have never been greater. Unfortunately in recent years, academic institutions expend exorbitant amounts of time and resources on the quantifiable areas of engineering; leaving the subject of engineering design relatively unaltered.

In the past, computational power was limited and therefore restricted the abilities for high fidelity analysis (three dimensional flow and structural analyses). Currently, the computational power required to run a full suite of complex FEA and Reynolds averaged Navier-Stokes (RANS) CFD codes is available from a common desktop workstation. As a result, present-day practice is no longer limited by computational power, but by the aircrafts geometrical definition [3]. Currently, large U.S. aerospace manufacturers primarily represent their aircraft geometries using surfaces. This method has worked in the past; however, with the advancements in computation, 1000's of aircraft can be analyzed in a matter of days. The problem with surface representations is they require tedious stitching between adjacent sheets. This process is done manually, requiring many engineering man hours to complete. After the geometry is completely air-tight, it can be gridded, meshed, and simulated. It would (and does) take years to analyze a comparable amount of these surface configurations that can otherwise be done using solid geometry; because solids do not require weeks of surface stitching.

The aerospace industry has experienced significant changes in the product development time. The question may be asked, with the advancements in modeling and simulation time, why have product development times increased? For example, the Lockheed F-117 stealth aircraft was designed, built, and put into operation is 5 years. The F-35 joint strike fighter request for proposals (RFP) was issued in the early 1990's and the aircraft is still not fully operational. There are many theories as to why the development time has escalated, including greater complexity and increased risk management. While these theories deserve merit, an underlying problem exists in the aerospace industry – absence of a seamlessly integrated design process.

Advantages of a fully integrated design process were recognized by the automotive and consumer goods industries in the 1990's. Automotive development time was reduced

from 6 to 3 years. In the 2000's, further advancements reduced the product cycle time from 3 years to 18 months. Changes in design processes for these industries were prompted by competition from foreign markets. The aerospace industry is at a cross road. If the industry continues along its current path, key segments of its traditional markets may be lost to foreign market competition.

2.2 Design Methods

2.2.1 Historical

The basic design process has been around since the 1400's while erecting the Florence Cathedral (Santa Maria del Fiore) [4]. It begins with an initial conceptual design and then progresses through concept evaluation, detailed design, process planning, manufacture, and assembly. The first two stages of this process mainly relied on pencil, paper and physical prototypes up through World War II and the 1970's [4] when engineers began using computers to aid them in the design process.

2.2.2 Brief History of Computer Aided Engineering

In the 1960's computers became powerful enough to facilitate solutions to problems that were previously only possible by hand. Structural mechanics industries are among the first disciplines to take advantage of the computing power using finite element methods. Finite difference codes are also implemented for fluid mechanics using idealized geometries. SKETCHPAD, developed by Ivan Sutherland at MIT and DAC-1 (Design Augmented by Computers) from General Motors, introduce the first CAD programs.

By the 1970's and 1980's higher level computer languages make it possible for CAE (computer aided engineering) tools to develop graphical user interfaces. This is also a time when it becomes common practice to use structural codes for validation. Complex surface modeling became standard late in the 1970's and Boeing along with General Electric are commissioned to develop a standard file format for representing three dimensional objects by the Department of Defense (DoD). This new file format is known as Integrated Graphics Exchange Specification (IGES) and is the standard file format for all government contracts. In the late 1980's, engineers working on the National Aerospace Plane (NASP) pictured in Figure 2.1 used full nose to tail geometric surface representations in their analysis.

Figure 2.1: National Aerospace Plane.

Early on in the 1990's CFD begins to emerge as a viable option for solving complex three dimensional geometric representations [5]. This is also the decade when three-dimensional parametric solid modeling begins to transform CAE processes by seamlessly integrating CAD geometries into analysis. The automotive industry is among the first adopt a process where geometries are able to be transferred directly from CAD into a simulation environment. These unified parametric vehicle (UPV) models are solid body CAD geometries with parameters that adjustment based on analysis results to improve performance [6]. Figure 2.2 shows the flow field on a plane bisecting a UPV during a simulated wind tunnel test. It can be seen in the left image that the entire facility is modeled to more precisely correlate simulation results to test data. The model is an assembly of smaller components which are parametrically coupled to create a single coherent model.

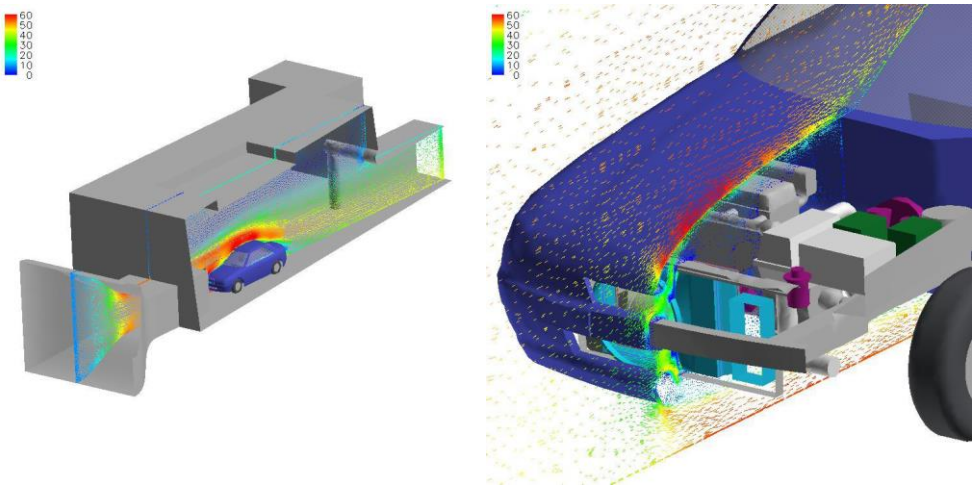

Figure 2.2: Ford Motor Company UPV simulation in a wind tunnel [6].

This CAE process was not only capable of capturing the complex component interactions of the exterior, but could also monitor the interior cabin thermal comfort level of human manikins. Figure 2.3 below illustrates the solid model representations of the cabin and a simulated interior environment.

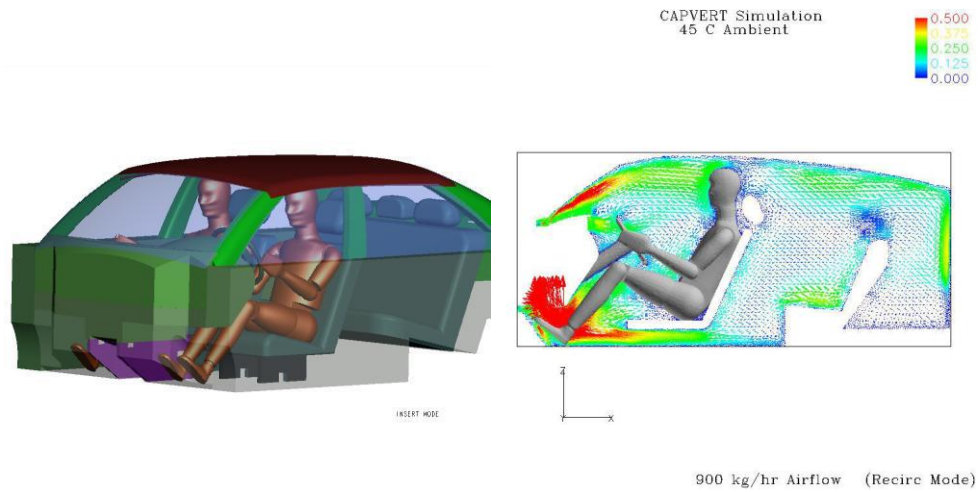

Figure 2.3: Interior cabin thermal comfort model (left) and simulation (right) [6].

By the turn of the century in the early 2000's, consumer goods adopted a simulation based design (SBD) process. Among these companies was Whirlpool Corporation. The engineers at Whirlpool extended simulation based design into include the complex interactions of multidisciplinary design. Modeled interactions encompassed design down to the component level up through manufacturing and packaging [7]. Increasing the degree of modeling complexity allowed multiple design teams working on separate components and subassembly modules to use the same master assembly. Figure 2.4 displays working system modules and components as separate parts of a larger master assembly.

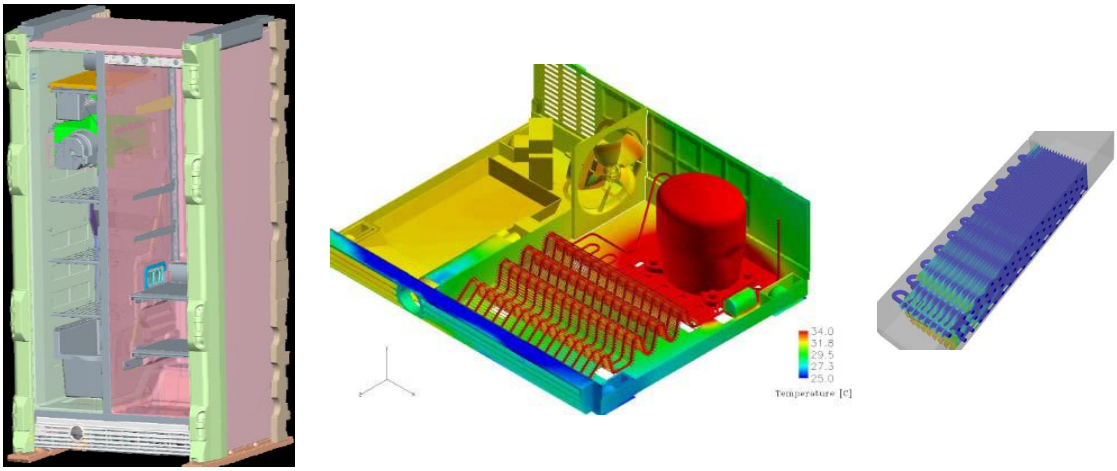

Module System Master Assembly | System Module Set validation for Thermal Requirements | Evaporator Module Performance Validation

Figure 2.4: Refrigeration systems incorporated into Whirlpools SBD process [7].

The top down design process allowed Whirlpool to assess the impacts design changes made not only between components, but effects to the supply chain as well. Capabilities to asses packaging was also included to compare the capital required to increase the structural steel of the appliance vs. increasing the waste packaging materials used to secure the appliance during transportation.

2.3 Top Down Design Methodology

A top down design (TDD) method uses system requirements as the highest level of design criteria. System requirements are defined by customer requirements, regulatory requirements, business requirements, and even societal. These requirements are translated into vehicle requirements and characteristic features by engineering design teams to drive a conceptual model. Once a conceptual model is established, preliminary design begins. Using the conceptual model as a template, system features are integrated and parameterized. By having all design groups work from a common CAD model, design modifications can be traced down to all their dependent systems. Each level of the top down design method is detailed in the sections to follow.

2.3.1 Requirements

Every design variant is scored against the top level system requirements. Requirements fall into three primary categories: 1) Customer, 2) Regulatory, and 3)

Business. Customer requirements may specify a minimum range, maximum speed capability, acquisition price, and/or payload capacity. The Federal Aviation Administration (FAA) sets many regulatory requirements on environmental impacts (emissions, noise, etc.) and safety (fire precautions, ventilation, collision avoidance, etc.). Many associations exist between customer and business requirements, however, from the business perspective, profit and operational costs are often a main concern. The fourth system level requirement is societal. These requirements are often times based on ethics and impacts to humanity.

In order to translate between requirements and vehicle performance targets, design engineers frequently utilize a quality function deployment process (QFD). This tool facilitates the transition between phases all the way down to component level design by defining potential options for how requirements can be accomplished. An example of a QFD is shown in Figure 2.5.

Row #	Max Relationship Value in Row	Relative Weight	Weight / Importance	Column #	1	2	3	4	5	6
				Direction of Improvement: Minimize (▼), Maximize (▲), or Target (x)	▼	▲	x	x	x	▲
				Quality Characteristics (a.k.a. "Functional Requirements" or "Hows") / Demanded Quality (a.k.a. "Customer Requirements" or "Whats")	TSFC	L/D	Fuel Volume	Statically Stable	Dynamically Stable	(Total Volume) - (Fuel Volume)
1	9	23.1	9.0	Cruise Mach	⊙	⊙				
2	3	15.4	6.0	GTOW (Air Drop)			○			○
3	9	23.1	9.0	Stable				⊙	⊙	▲
4	9	23.1	9.0	Range	⊙	⊙	⊙			⊙
5	9	15.4	6.0	Payload			⊙		▲	⊙

Legend		
⊙	Strong Relationship	9
○	Moderate Relationship	3
▲	Weak Relationship	1
++	Strong Positive Correlation	
+	Positive Correlation	
−	Negative Correlation	
▼	Strong Negative Correlation	
▼	Objective Is To Minimize	
▲	Objective Is To Maximize	
x	Objective Is To Hit Target	

Figure 2.5: Simplified QFD chart and legend.

A QFD assists in tracking design performance by weighting the importance imposed on each requirement and assigning relational values (see legend in Figure 2.5) between each requirement to be met and the possible range of solutions. Cross correlations are determined in a matrix above each potential solution. This diagonal matrix is analogous to a roof and the intersections below it are representative of a house. QFD processes generally contain several houses of quality where, for each increasing level, the functional requirements become the new demanded qualities.

2.3.2 Conceptual Concurrent Design

Only evaluates designs on the vehicle level. Scoring is based primarily on fundamental flight performance metrics, structural evaluations, FAA regulations, and cost estimates. Scoring is weighted by the established requirements from the QFD's 1st House of Quality. A simplified flow diagram for a top down approach to conceptual concurrent design is illustrated Figure 2.6.

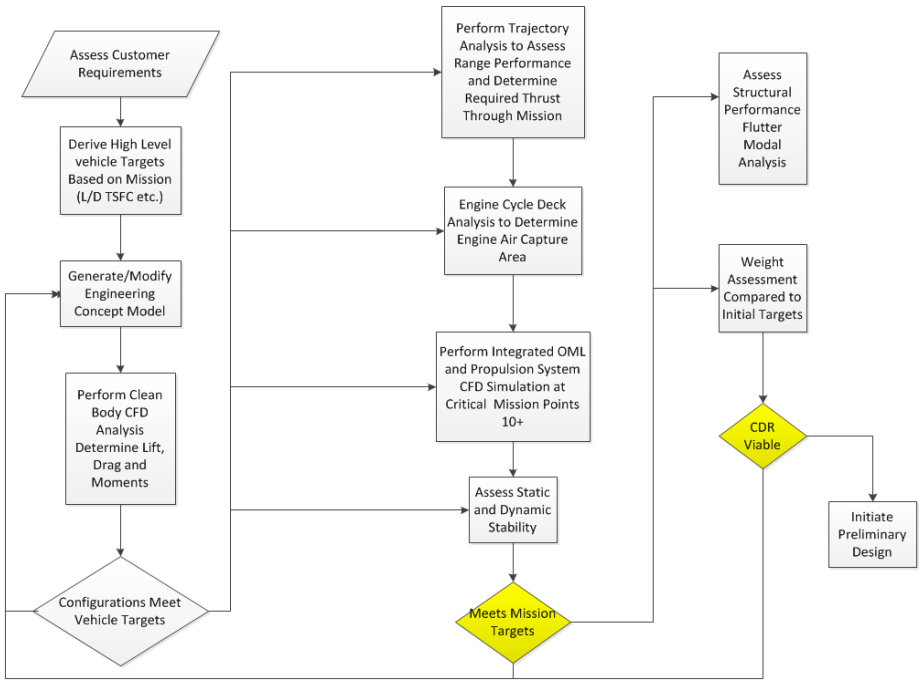

Figure 2.6: Conceptual design flow chart.

The four concurrent performance assessment blocks in Figure 2.6 are preceded by verification of vehicle targets. This step determines which configurations are viable candidates for more detailed analysis. After the performances are assessed, they are measured in terms of the mission. If the mission targets are met, the design passes on to weight assesment and structural analyses. If structural and weight analyses reveal a viable design, the configuration is subject to a conceptual design review (CDR) before passing through to preliminary design. If a vehicle falls short of mission targets or fails its CDR, the engineering concept model is modified and reanalyzed.

The engineering concept model contains all relevant design parameters for each engineering design discipline. During the conceptual design phase, parameters are relatively simple and are constrained to the outer mold line (OML), propulsion system, stabilizers (with

control surfaces), packaging volume, and system placement. Figure 2.7 below details typical department relations a concept model supports.

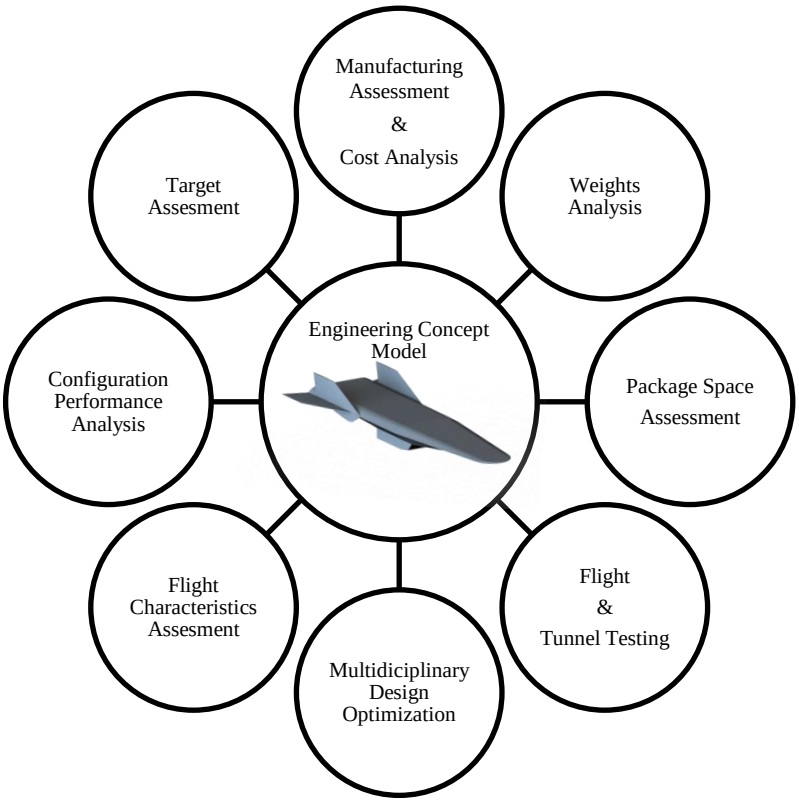

Figure 2.7: Sample diagram for a CAD-centric design environment.

Because the conceptual design model is constantly fluctuating, it is important each department works from this common model. This ensures all design groups are aware of modifications and are working from the most current design model. All conceptual design iterations retain their respective concept model; linking each performance score to a representative CAD model. This capability serves as a detailed design history for each modification. Performance can be tracked in many ways; however, a simple method is a design scorecard. A design scorecard ties the vehicle back to mission requirements and enables engineers to monitor vehicle convergence. This can be done simply by using red, yellow, and green color coded blocks to represent quantified targets. Figure 2.8 illustrates an example scorecard with the targets arranged down the first column and each design variant across the top.

		Vehicle Variations					
Conceptual Vehicle Targets	Baseline	V_01	V_02	V_03	V_04	V_05	V_06
Mach 5 Cruise L/D > 6.5	6.21	6.77	6.51	5.87	6.35	6.49	6.32
Lift > 10,000 lb GTOW	9,785	10,046	11,729	7,890	9,360	11,670	10,526
Range > 2500 nm	2308	2248	2412	2387	2621	2346	2155
Positive Static Margin	Y	Y	N	Y	N	Y	Y
TSFC < 3.0 at Cruise	N	N	Y	Y	Y	Y	N
Inlet Distortion < 5%	N	N	Y	N	Y	Y	Y
Inlet Pressure Recovery > .96	0.85	0.91	0.81	0.88	0.92	0.94	0.95

Figure 2.8: Example of a conceptual design scorecard for multiple vehicle variations.

The vehicle targets have a numerical value that qualifies a variation for either meeting a target or failing. Variations that meet the specified target are represented with green shaded cells. Failure to meet a target is represented by red cells. Yellow shaded cells fall somewhere between the lowest scoring variation and the indicated target value. The example above uses numerical results to determine shading. Other methods may strictly use integer scale values such as 1 through 10 or 1 through 3.

2.3.3 Preliminary Concurrent Design

The highest performing design which meets or exceeds targets from the conceptual stage is selected to enter into preliminary design. Subsystems are included into the engineering concept model such as landing gears, control systems, structures, and refined weight assignments. The CAD model also maintains nearly all previous capabilities to modify design parameters. Experts in their respective areas increase the level of design detail for each system. Preliminary design is also when fabrication begins for correlating analytical models with physical models. These can include wind tunnel models and some structural members of interest. Physical testing also increases confidence in the analytical models. CFD and FEA models have considerably increased fidelity compared to conceptual analysis simulations. Multiple system integration trade studies and optimization routines incorporated into preliminary design exploits many residual performance gains from the conceptual design process. Nearly all systems and performance metrics from the conceptual design phase remain integrated in the scorecard to maintain design change traceability. Scorecards include the subsystem performance metrics to accommodate subsystem requirements.

2.3.4 Detailed Design

After all systems and subsystems have been established, design at the component level begins. During the detailed design phase, the vehicle configuration is deemed viable

and meets all requirements. Tasks completed include: interior layout, shop drawings, and placement of hydraulics, electrical, fuel lines and ducting. Typically design for manufacturing is also completed at this phase in the design process [2] such as tooling equipment and jig arrangements for component production. By this point, it is important that design changes be kept to a minimum, as the cost to modify components can be substantial depending on the number interactions there are with other systems, subsystems, and components. Often times, shop drawings are verified and released early for certain components so fabrication may commence. Changes made to components already in production can have crippling effects to project deadlines and budget. The earlier adverse interactions can be caught, the less chance there is for costly modifications during detailed design. Increasing the fidelity of the conceptual model and using a top-down-design methodology, the probability of exposing adverse interactions increases dramatically for hypersonic aircraft.

CHAPTER 3. INTELLEGENT CAD MODELS

When considering a CAD-centric approach, there are three important considerations that need to be addressed within the CAD Model itself: 1) Operability by other design groups, 2) Intelligent relations between features, and 3) Robustness and flexibility. A CAD model with these characteristics will hence forth be referred to as an iMod (intelligent Model). When iterating through preliminary design cycles, iMods improve efficiency by minimizing undesired side effects from the modification of design variables.

A simple example to consider is increasing/decreasing the inlet capture area of an engine nacelle. If a relation is created between the feature sketches (see section 3.2.1 for CAD too definitions) that control the capture area for the flow path and the feature sketches which control the outer diameter of the engine nacelle, when one dimension is altered, the others will maintain a constant specified distance. Figure 3.1 shows this update relation by setting the outer nacelle diameter equal to the inlet diameter + 2 inches. Relations of this type reduce the number of dimensional changes required to update geometries and preserve geometric relations. Using the same example in Figure 3.1, if the relation described is not applied and the inner diameter was decreased from 36 inches (left) to 24inches (right) the resulting geometry would have an engine nacelle leading edge radius of 3.5 inches rather than the initial designed radius of 1 inch.

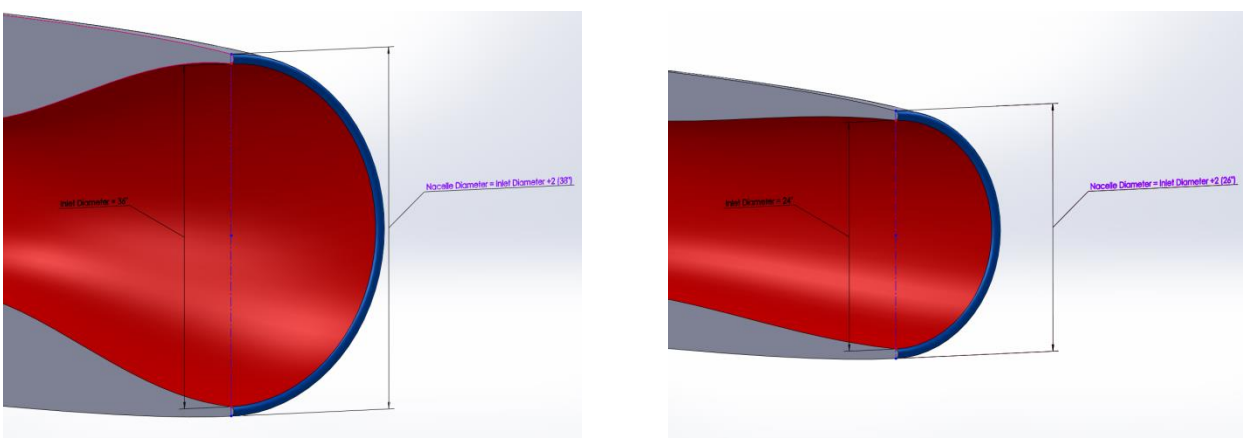

Figure 3.1: Intelligent relation between inlet capture area and outer nacelle diameter.

Other, more complex relations that could only be realized by a practicing engineer define the intelligent relations. An example of an intelligent relation would include considerations for vortex shedding and wake interactions between upstream and downstream

features. Another important aspect of an iMod is all solid features are merged to form a single solid body; thus creating a manifold geometry.

It is important to have air-tight geometry when analyzing performance using Computational Fluid Dynamics (CFD). By definition, a solid body is air-tight and will create a single manifold geometry with the air domain when Boolean operations are executed. A difficulty of using surfaces for complex geometry is they are inherently discontinuous and must be sewn or stitched together before they can be properly gridded and meshed. If gaps exist in the aircraft, the boundary conditions at those locations are absent and the air domain is allowed access to the interior of the outer mold line (OML). If that occurs, at best, the residuals will not converge. More commonly, surface gaps prevent the geometry from being discretized into a grid for meshing. Solids are also beneficial when defining a location for the center of gravity (C_g). By using mass properties, weights can be assigned to individual components and located within the OML domain to position the C_g for aircraft stability.

3.1 Initial Sizing and Design

From provided mission requirements, target L/D ratios and volume constraints are set. Using the targets, preliminary designs are proposed to meet the specified requirements. No initial design is perfect, which is why incorporating parametric capability into beginning concept models is important. For supersonic/hypersonic aircraft such as the Lockheed D21-B, Blackswift (HTV-3) from DARPA, and NASA X-43, configurations are typically lifting bodies or blended wing body aircraft. Length scales vary from as little as 3.7 m for NASA's X-43 [8] to just over 13 m for the Lockheed D21-B [9]. Keeping within these bounds set by legacy aircraft, a proposed initial design model 10 m in length is selected as an appropriate size for the case study in Chapter 5.

3.2 Construction Methodology Overview

3.2.1 CAD Tool Definitions

In order to effectively discuss construction methods, some common CAD tool definitions must first be made. SolidWorks 2014 is the primary modeling software used in the creation of all iMods in this chapter and the chapters to follow.

Construction/Reference Line

These are lines used for creating references within the design domain. Construction lines create the foundation on which OML features are built from and control all parametric variations. Nearly all feature sketches and guide curves in the following sections will

reference construction lines. The terms construction line and reference line will be used interchangeably throughout this study.

Loft Features

A CAD tool used to create or remove solid regions between two or more feature sketch profiles. If no control criteria are set, the loft will interpolate cross sectional transitions between the feature sketches.

Feature Sketch

Is a sketch that is commonly used by loft and extrude features to define the bounds for the OML and other aircraft components. If using feature sketches for lofting, robustness can be improved by using the same number of line segments in each feature sketch and including guide curves between the sketches.

Sketch Plane

Used as datum for creating sketches. These reference geometries can be created using a multitude of different techniques; however, some methods are better suited for certain applications. For example, if the goal is to create a control sketch for wing dihedral, then the simplest reference set would be a plane with a parallel constraint to the front plane and horizontally dimensioned point that is coincident with the centerline. The same plane could have just as easily been created with a perpendicular constraint to the mirror plane and a coincident constraint to a vertical line sketched on the mirror plane.

Guide Curve

User defined sketches to control loft contours. They can be a single line or curve and/or a combination of lines and curves in a series. When using guide curves to create loft features, they must intersect all feature sketches within the loft domain. Model edges may also be used as guide curves, however, for robustness it is not recommended. This is because model edges may disappear depending on dimensional combinations within the configuration design – resulting in a broken reference and possible failure to regenerate the feature.

Spline

When fitting a spline to predefined construction line endpoints, by default it will assume a fit using multiple 3rd order polynomial segments. These splines are known as b-splines. Handles provide user defined tangency control. Increasing the magnitude of a spline handle increases the tangency strength from its respective spline point. For more robust spline control SolidWorks 2014 includes style splines which are based on Bezier curves.

Although this spline type is more robust, it does not offer the exact point to point intersections available from b-splines.

Model Hierarchy

Two basic terms are commonly used to denote the hierarchy in a CAD model – "parent" and "child". A feature or sketch used as a reference for creating another is known as a parent feature. A feature or sketch that references another is known as a child of the referenced feature or sketch. This is the foundation on which parametric models are built. Using an edge or vertex of a solid body is not a recommended parent reference for the same reason noted in the "Guide Curve" section above.

Figure 3.2 through Figure 3.4 illustrate the parent-child relations between three sketches (S*) and four sketch planes (P*): S1) Centerline, S2) Height Control, S3) Anhedral/Dihedral Control, P1) Mirror, P2) Front, P3) Mid, and P4) Rear. The front (YZ) and mirror (XZ) planes are fixed in space and represent the models absolute coordinate system. The *Centerline* sketch is attached to the mirror plane and is therefore dependent on it. The sketch titled *Height Control* is coincident with a point on the centerline sketch and is drawn on the mirror plane. This creates a dual parent relationship; one with the centerline and another with the mirror plane. The rear and mid planes are parallel with the front plane and coincident with points on the centerline. The sketch labeled *Anhedarl/Dihedral Control* is drawn on the mid plane and coincident with the sketch titled height control. By creating these relations, anhedral/dihedral control is entirely dependent on its own dimensions and the parent features it references. For each succession through the following figures, a different parameter is altered to better demonstrate the parent-child relations. Figure 3.2 shows the initial positions for each model feature.

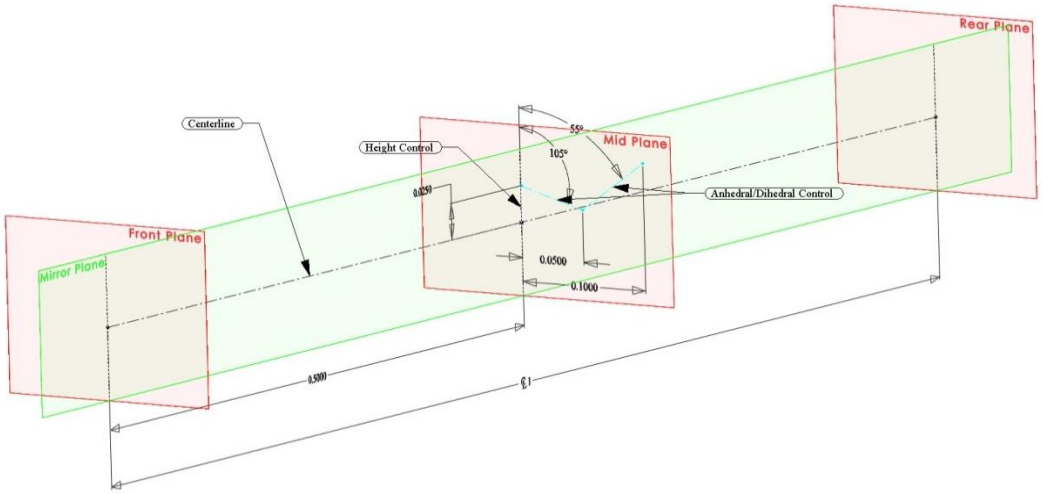

Figure 3.2: Parent-child relationships. Original sketch positions.

A dimensional alteration is made to a point on the centerline sketch in Figure 3.3. The point is referenced by the sketch "Height Control" and the Mid Plane. It can be seen that all child features and inherited child features (Anhedral/Dihedral Control) also translate with the point down the centerline. All other constraints not associated with the parent feature "Centerline" remain unaltered.

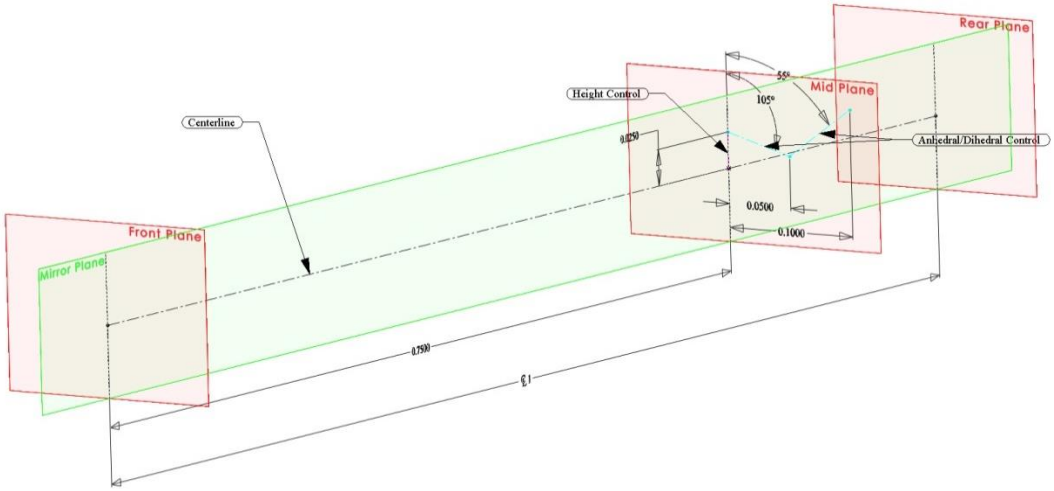

Figure 3.3: Parent-child relationships. "Centerline" sketch alteration.

Figure 3.4 shows the result of a modification made to the sketch "Height Control". This sketch is a child of the "Centerline" sketch and a parent to "Anhedral/Dihedral Control". Comparing Figure 3.4 to Figure 3.3, all construction lines of "Anhedral/Dihedral Control" have undergone a downward vertical translation.

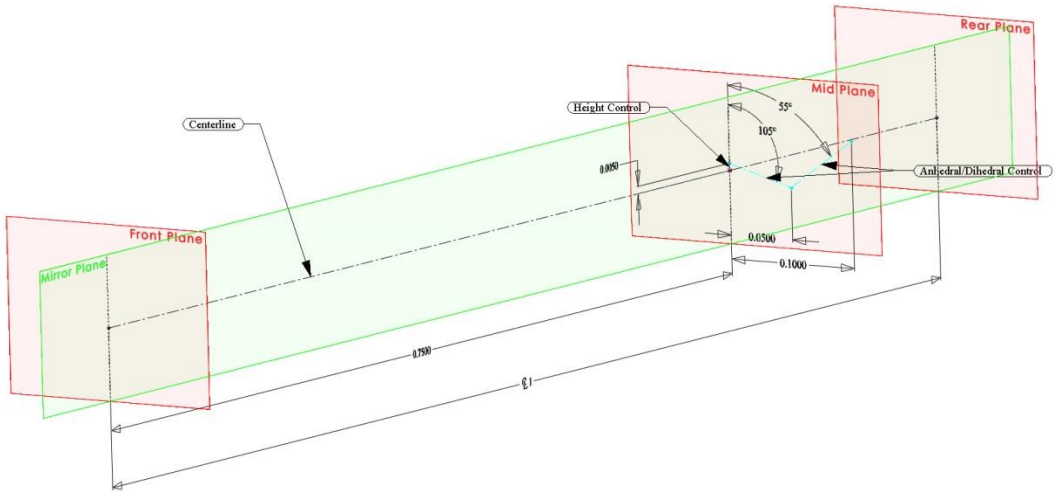

Figure 3.4: Parent-child relationships. “Height Control” sketch alteration.

It also follows that any dimensional alteration to the sketch “Anhedral/Dihedral Control” will only affect the lines within that sketch since it has no dependent children.

3.2.2 Simple Parametric Example

Features of parametric interest are built upon a foundation of construction lines which control and define feature positions within a three dimensional Cartesian coordinate system. Primary parametric features include overall aircraft vehicle length, cross section dimensions and absolute distance from nose for each cross section, wing dihedral, wing planform characteristics (section spans, chord lengths, sweep, etc.) and airfoil properties for each wing section. Below is a simplified example of how construction lines are used to create parametric variations for a loft between two rectangular cross sections.

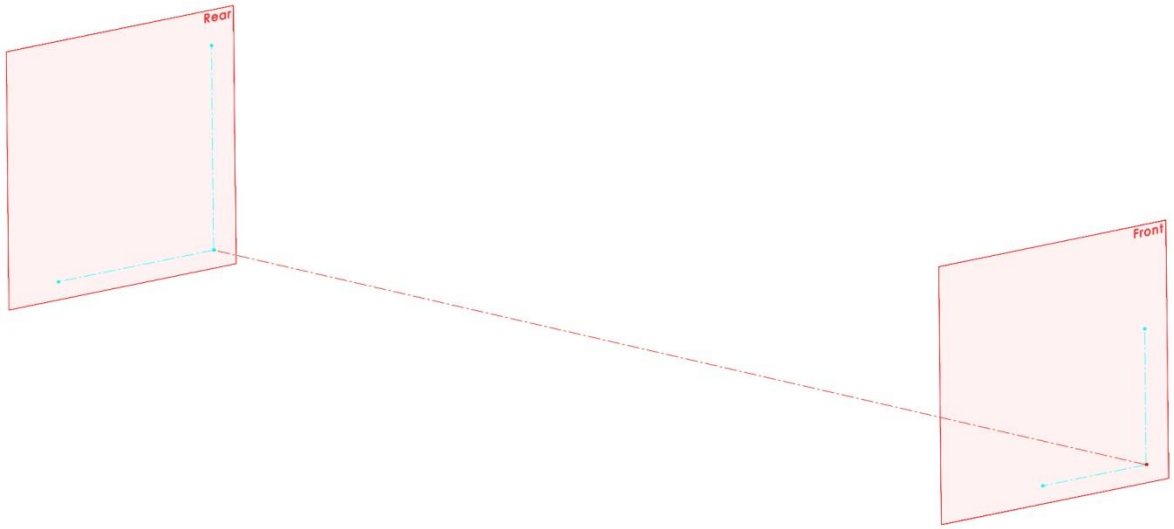

Figure 3.5: Simple example of iMod parametric control sketches.

The origin is used as reference point to fix features in space and is located where the red dashed line intersects the front plane. The red centerline is used to control the overall length extending down the –X axis (in a stability coordinate frame) and references the origin. The front and rear sketch planes are used to create the front and rear cross section construction lines (cyan dashed lines) and body feature sketches (blue solid lines) in Figure 3.6. The vertical cyan line on the front plane is directed along the –Z axis and the horizontal cyan line along the +Y axis. These directions are representative of a body fixed stability coordinate system.

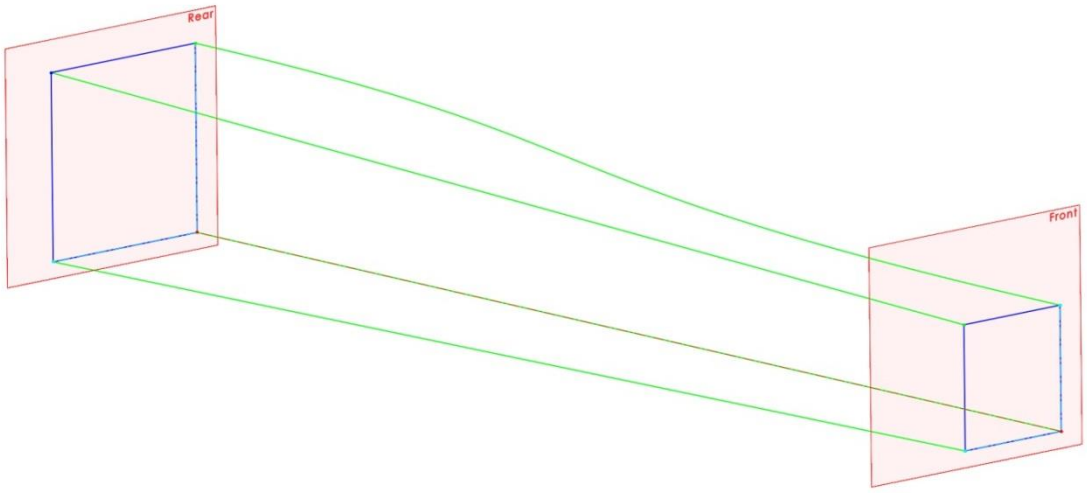

Figure 3.6: iMod with body cross section sketches and guide curves included.

The body cross section sketches (blue) are children of the cyan colored body cross section construction lines. The guide curves (green) are children of both the cyan body cross section construction lines and the blue body cross section sketches. By arranging the model hierarchy as such, dimensional variations in the cyan and red parent construction lines will cascade down the feature tree to all their children (rear plane, front and rear cross sections, guide curves, and the solid body loft). Several variations are illustrated in Figure 3.7.

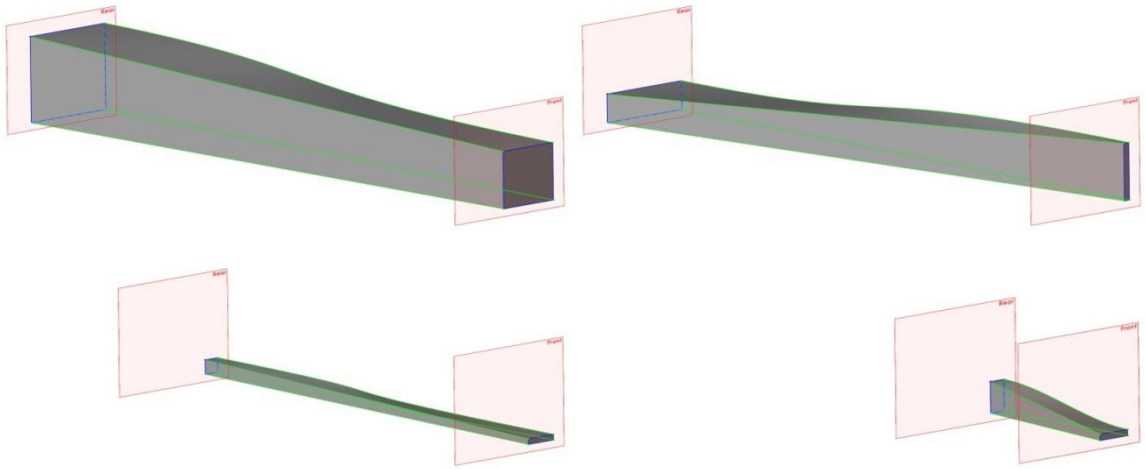

Figure 3.7: Simple loft variations between two rectangular cross sections.

All green guide curves are straight lines with the exception of the upper curve located on the XZ plane; which is a spline with handles at each endpoint. Each handle of this spline is driven by an equation setting the tangency magnitude equal to 50% of the centerline length. The baseline configuration is represented in the top left. Variation 1 (top right) has

deviated from the baseline by only the front and rear cross sections. Variation 2 (bottom left) has a 25% reduced length and altered cross sections. Variation 3 (bottom right) is reduced 75% in length and also has altered cross sectional aspect ratios.

3.3 iMod Construction Process

Depending on the class of aircraft, the construction process of iMods will vary. In the following sections two aircraft are considered; 1) A blended wing body (BWB) configuration for an air breathing hypersonic vehicle and 2) A traditional aircraft configuration for a supersonic business jet. The first step necessary to constructing any iMod is determining which design parameters are of interest. Each design group will have individual goals and targets which must be addressed within the iMod. Therefore, determining the dimensions and aircraft characteristics for parameterization is a deliberative process between groups.

3.4 Blended Wing-Body Aircraft: Hypersonic Wave Rider

Due to the nature of blended wing bodies (BWB), it is difficult to use multiple loft features and create a smooth wing-body transition. Because of this, the design engineer must be creative when constructing a parameterized model. One such technique that provides exceptional control is point-to-point transitions. This method consists of multiple cross sections distributed longitudinally down the centerline. Each of these cross sections has driving construction sketches for span, anhedral/dihedral, and thickness. Section 3.4.2 provides details for constructing this model type.

3.4.1 Design Parameters

Point-to-point control offers parameterization for a very diverse set of OML features; however, there are other design variables which can be built into an iMod that offer more broad control. An example of broad range feature control is constraining the points defining the leading edge (LE) to a single construction line. This can be a useful technique to force the model to have a linear leading edge or to drive the wing LE by a Mach cone relationship. Stability parameters may also be incorporated into the reference sketches that drive the vertical stabilizer(s) and trailing edge control surfaces.

Ramp Angles

For air breathing hypersonic aircraft with inlet positioned below the body, the upstream ramp angles play very important roles in propulsive efficiency. To compress the air before entering the inlet, a series of shock waves are generated at each ramp transition [10]. At the design Mach number, the oblique shock structure should resemble Figure 3.8

and converge on the inlet cowl lip. The fuselage reference line is defined being parallel with the flow when the aircraft is at zero degrees angle of attack. Ramp half angles used to determine the shock structure are depicted in Figure 3.8 as θ_1, θ_2, and θ_3.

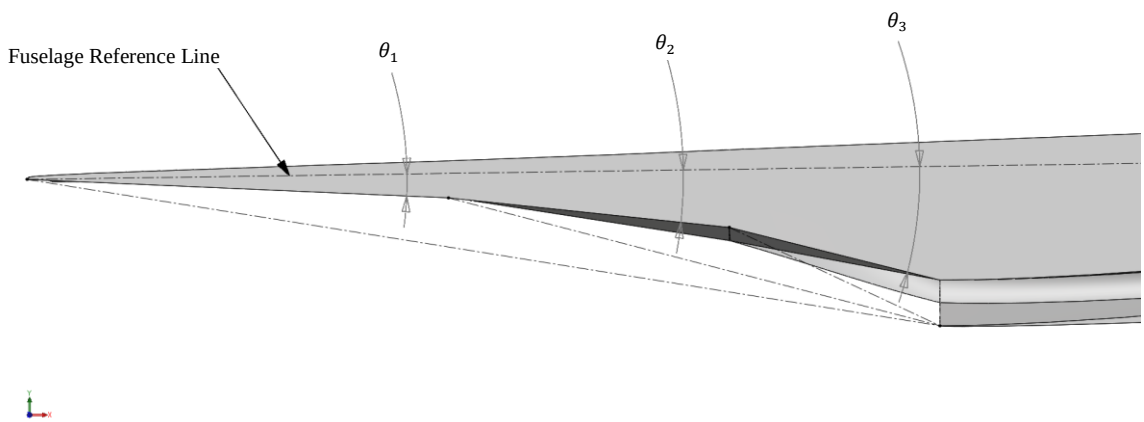

Figure 3.8: Design approach to ramjet/scramjet inlets at design Mach number.

Having parametric control over the half angles gives engineers the capability to quickly determine the best set of angles for the designed cruise condition and accommodates any necessary changes later in the design process. The same concept may be extended to variable geometry inlets and nozzles.

Leading Edge-Mach Cone Relation

Hypersonic wave riders are characterized by matching their leading edges up with the cruise condition Mach cone. By doing this, the shock cone produced by the nose attaches to the LE and isolates the low pressure region above from the high pressure region below. An example of this phenomenon is pictured in Figure 3.9. Absolute pressure contours are displayed on a plane that laterally bisects the aircraft and fluid domain. Red, orange and yellow indicate high pressure regions. Shades of blue indicate low pressure regions. Shades of green represent pressure values which are near to the atmospheric pressure.

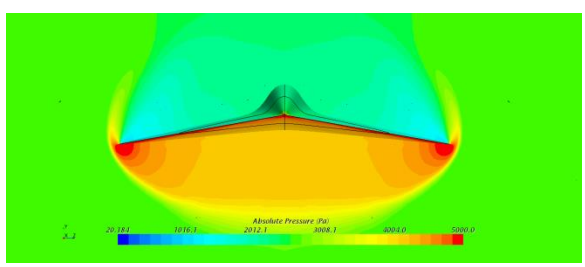

Figure 3.9: Mid-plane high and low pressure contours.

Stabilizers

Due to the nature of a BWB configuration, a horizontal tail is not a necessary or appropriate component. To accommodate the eliminated stabilizer, control surfaces are can be positioned along the trailing edges of the wing. Yaw stabilization can be achieved through a body centered vertical tail, symmetric twin tail, or by oversizing the winglets. Structurally, vertical stabilizers on the wing tips are not as viable as body centered or twin tail configurations. Aerodynamically, a vertical stabilizer centrally located on the body becomes "shadowed" at hypersonic speeds from the wake created by the nose at even small angles of attack [11]. This dramatically reduces the effectiveness for body centered stabilizers. Symmetrically offset vertical stabilizers with a slight toe-in provide an aerodynamic and structural compromise between the two configurations.

Control Surfaces

After completing the conceptual design process, higher fidelity characteristics can be incorporated into the iMod. Usually for aircraft showing a high performance index, control surface deflections are analyzed. Elevons are a common example of this and provide the functions of both an aileron for roll and an elevator for pitch control.

3.4.2 Construction Process

The beginning foundation for constructing a blended wing body aircraft resembles the example of section 3.2.2. First reference lines and planes are made. After that, feature sketches are attached to the reference geometry, and finally lofts are made between sections. Figure 3.10 shows the coordinate system used throughout the construction process and includes two reference lines at the origin. One line extends along the y-axis and represents the right wing direction; the other is aligned with the negative x-axis and designates the special location for the aircraft body. The nose of the aircraft is coincident with the origin.

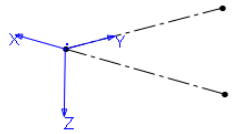

Figure 3.10: Reference coordinate system.

Longitudinal Control Sketches

Similar to the traditional aircraft in section 3.5, a centerline is created to establish a fixed reference line for body control parameters. Constructed on the mirror plane and

beginning at the origin, the centerline extends down the negative x-axis. The length of this line determines the total length of the aircraft. Coincident points are added to the centerline. Each point represents the longitudinal position of a body cross section and is dimensioned from the origin. Also included in the centerline sketch are angle controls for each body cross section which provide variability in the vertical direction. To begin, a single reference line is made coincident with the origin extending vertically upward along the -z axis and dimensioned. This dimension will define the leading edge radius for the wing. Next, a chain of lines are created beginning at the free end of the LE radius reference line. The number of line segments in the chain should equal the number of points on the centerline and terminate at the endpoint of the center line. Small vertical lines are created at the endpoints of each line segment. Each is constrained to a vertical orientation as well as a midpoint constraint. These construction lines are used as a reference line for dimensioning the body section angles. Figure 3.11 shows the current model state up to this point with arbitrary dimensions.

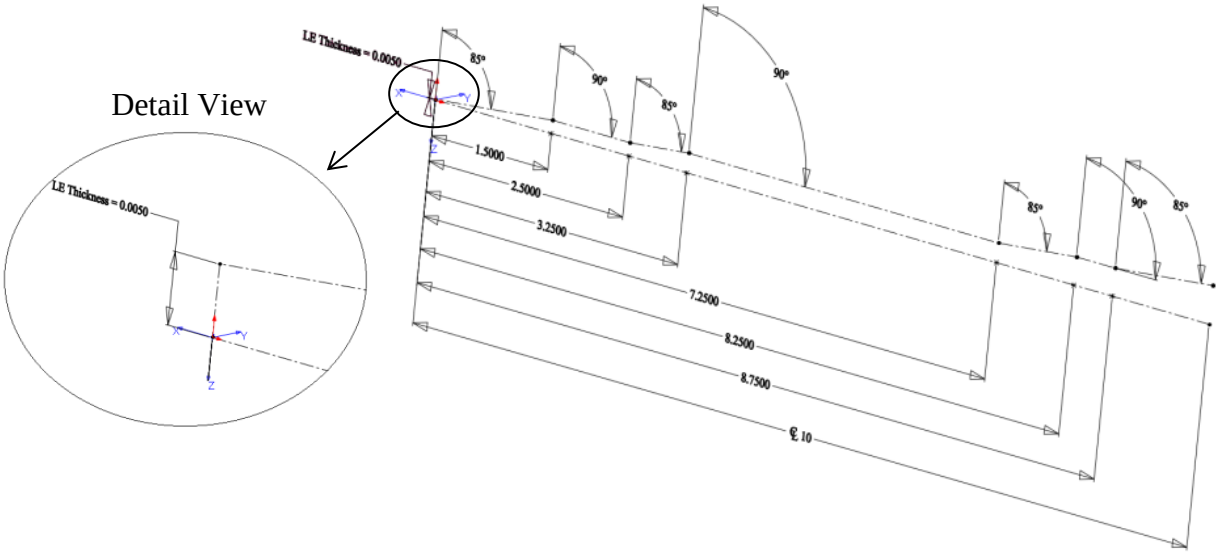

Figure 3.11: Centerline body section angles. Detail view of nose LE thickness control.

A second reference sketch is created on the mirror plane to control center thickness of each body cross section. Two vertical construction lines are created at the endpoints of each line segment. One line extends upward and the other line downward; both are given vertical constraints and dimensioned relative to their respective endpoint. If it is more desirable to drive the lower forebody with ramp angles to control the shock interactions with the cowl lip (see Figure 3.8) then the lower vertical lines can be driven using angles between the centerline section line segments and newly created lines that span from endpoint to endpoint on the lower vertical lines. Figure 3.12 displays the thickness control sketch in cyan. This

model also incorporates the ramp angles as a design parameter to drive the lower first three sections.

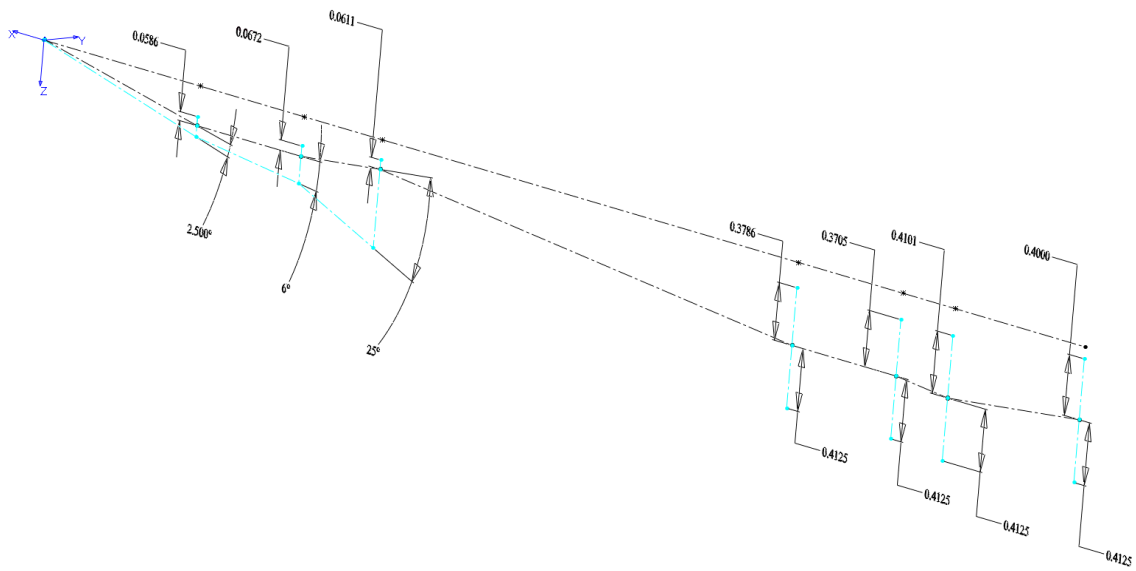

Figure 3.12: Body thickness control reference sketch (cyan) and centerline sketch (black).

Sections are numbered based on how many stations exist within the conceptual model developed by the design team. Stations are determined by regions of significant change; such as a ramp or variation in wing span. To begin with, station dimensions are added to the iMod to create similar proportions to the conceptual model; exact values may be entered at a later time.

Lateral Control Sketches

Now that longitudinal control has been established, lateral dimensionality is possible. Cross section planes are generated lengthwise, and for the purposes of this study, reference the fixed front plane (parallel) and centerline points (coincident). Each plane that references a centerline point becomes a child feature of the centerline, and therefore dependent, on the point. Every dimensional modification to the point moves the plane and every sketch on that plane. These planes contain the foundation on which all lateral dimensionality is built on.

Lateral control reference sketches are constructed on the cross section planes and have individual control over span, dihedral, and thickness. Assembled similarly to the longitudinal control sketches, each cross section control sketch originates off a common origin. To ensure robustness, the same point used as a reference for the sketch plane is used as the control sketch origin. Figure 3.13 shows a detailed view of the sketches that form a single lateral control sketch at a single station. Span and dihedral dimensionality are

contained in a separate sketch apart from the thickness control – identical to the setup for longitudinal control. The cyan line in the figure is the height control line from the body thickness sketch. To reduce dimensional clutter, only the span wise dihedral measurements are shown. Other dimensions include horizontal distances for each black line segment from the origin, upper and lower lengths for each magenta thickness control line, and LE thickness. LE thickness is driven by the same dimension from the detailed nose view in Figure 3.11; allowing all LE thicknesses to be updated from a single dimensional change.

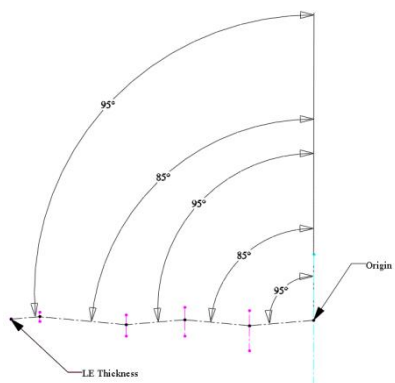

Figure 3.13: Lateral control sketches. Span and dihedral (black). Thickness (magenta).

To maintain consistent alignment between each span wise section, thickness lines are angled relative to the span segment that precedes it. To accomplish this, the two dihedral angles that surround it are averaged using Eq. 3.1.

$$\theta_{thick} = \left(\frac{\Gamma_{section\ 1} + \Gamma_{section\ 2}}{2}\right) - \Gamma_{section\ 1} + 90 \qquad \text{Eq. 3.1}$$

Where $\Gamma_{section\ 1}$ and $\Gamma_{section\ 2}$ are the inner and outer (respectively) dihedral angles relative to the vertical cyan body thickness control line. The resulting angle θ_{thick} is measured relative to the inner dihedral line segment ($\Gamma_{section\ 1}$) and drives the magenta thickness line.

A benefit of incorporating the average angle into an iMod is that even under extreme dihedral angles, the thickness angle will not bias toward eithier wing section. Figure 3.14 illustrates this biasing effect if not properly constrained. The magenta colored line furthest outboard (left) has a simple perpendicular constraint with the outside black dihedral line and is strongly biased toward the underside of the second (center) black line. The interior

magenta colored line is driven by Eq. 3.1 and remains centered between the surrounding dihedral reference lines.

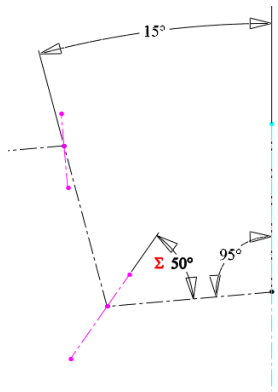

Figure 3.14: Lateral control sketches. Span and dihedral (black). Thickness (magenta).

After all cross section reference sketches are added, the iMod resembles the state of Figure 3.15. All black colored lines are part of the centerline sketch, green lines represent reference lines for body thickness and ramp angles, cyan is for the lateral span and dihedral control, and the magenta lines belong to longitudinal thickness control.

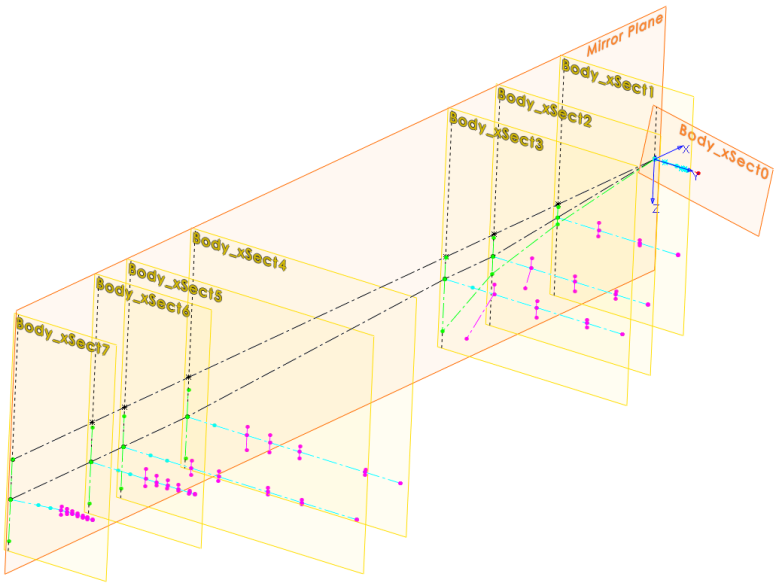

Figure 3.15: Display of all lateral and longitudinal control sketches.

Examining Figure 3.15 closer, it is evident that the magenta thickness control sketches on the planes “Body_xSect3” and “Body_xSect2” have interior line angles which

deviate from Eq. 3.1. This is to allow individual control over the ramp widths at those stations and is a useful technique for managing available surface area when sizing an inlet.

Feature Sketches

Little dimensioning is required for feature sketches even though they are what truly define the outer mold line at each station. These sketches are a result of their parenting control sketches and must be robust enough to regenerate under extreme conditions. Common failure modes include acute angles over short distances and unregulated tangency magnitudes for splines. For this reason, many of the feature curves on the wing are straight lines from point to point.

Feature sketches share transverse cross section planes with their parenting dihedral and span control sketches. Figure 3.16 illustrates the process of creating these feature sketches. To begin, a circular arc is added at the leading edge (a) and is governed by coincident relations with the LE thickness reference line. Second, lines are added between the endpoints of each upper and lower magenta reference line (b); leaving a gap in the first section. Lastly, splines are added to close the upper and lower openings and a vertical line (collinear with the mirror plane) encloses the boundary (c). The splines that form the first section are given start and end tangency constraints. These spline controls force a horizontal direction from the point lying on the mirror plane and parallel relation with the line that begins the second section from stage (b).

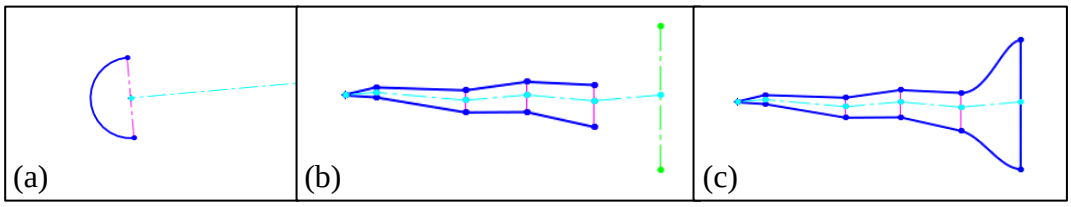

Figure 3.16: Progression through construction stages of a feature sketch.

For a more robust model, equations are added to control tangency strengths. Equations are set to have a linear correlation to the first wing sections span dimension; a decrease in span distance causes a decrease in tangency magnitude, the opposite is true for an increase in span distance. Having control of the tangency magnitude for curves increases robustness by allowing the spline to smoothly transition between stations by stretching and contracting rather than bending and kinking. It also provides consistency when modifying

design parameters. Figure 3.17 demonstrates how different spline control methods impact the outcome of a body feature sketch. The image to the left is a representation of the originally intended design form and has constant magnitude tangents in place. The center image is the result of reducing the first wing section span by 33% while preserving the constant magnitude splines. The drawing to the right also has a 33% reduction of the first wing section, but has all four spline magnitudes independently driven by linear equations which are dependent on dimensional span of the first section.

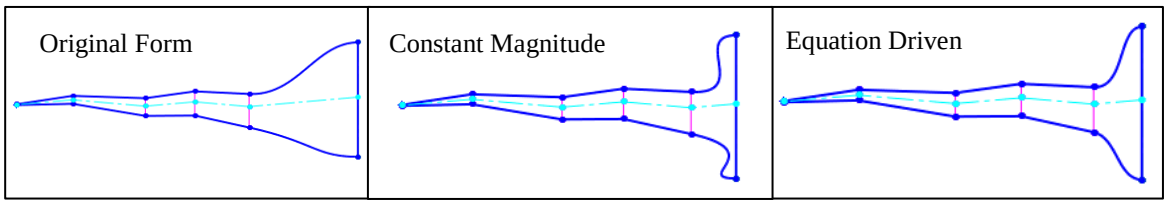

Figure 3.17: Tangency magnitude control comparison for body feature splines.

It is apparent to the design engineer that the constant magnitude outcome is less than desirable and adjustments must be applied. Rather than readjust the magnitudes every time the wing section has a span alteration, equations can be implemented to create the effect seen in Figure 3.17 (c). This is especially useful when implementing automated design optimization. One method is to establish the linear slope equation for the spline handles by simply determining feasible spline magnitudes for reasonably near and far wing span dimensions and use Eq. 3.2.

$$Magnitude = \left(\frac{M_{far} - M_{near}}{b_{far} - b_{near}}\right)(b - b_{near}) + M_{near} \qquad \text{Eq. 3.2}$$

Where M_{far} and M_{near} are the spline magnitudes at the arbitrary near and far span distances which produce the desired transitions, b_{far} and b_{near} are the chosen near and far span distances, and b references the current span dimension. This equation is the two-point slope form for a linear equation. Figure 3.18 shows all feature sketches (blue) added to the iMod. This is the display state for all wing-body features sketches. To ensure there are no errors within the model up to this stage, each set of feature sketches undergoes a section-by-section loft test.

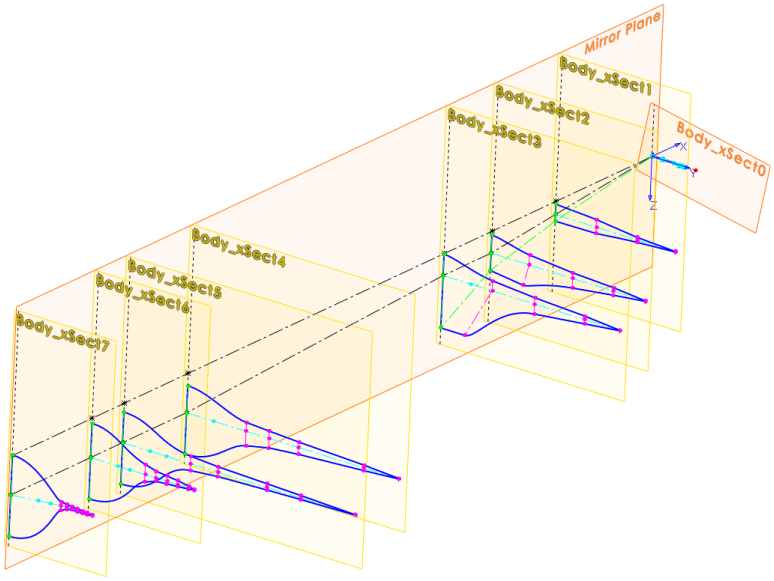

Figure 3.18: Model display state after all body feature sketches added.

Stabilizer

Vertical stabilizer sketches are constructed on their own independent planes and constricted to the body only enough to contain the root chord sketch completely within the OML. To enable twin tail configurations a transverse angle control relative to the mirror plane is incorporated. This reference sketch (red in Figure 3.19) is located on a transverse plane dimensioned longitudinally from the aircraft base. Control over the stabilizer planform is achieved using a series of construction lines (cyan in Figure 3.19) on a plane which references the transverse angle control sketch and the front plane (perpendicular relation). The root chord reference line is collinear with the second to last sections centerline to ensure complete submersion when it comes time to unite the solid features. The planform is driven using span length, chord length, and sweep angle dimensions.

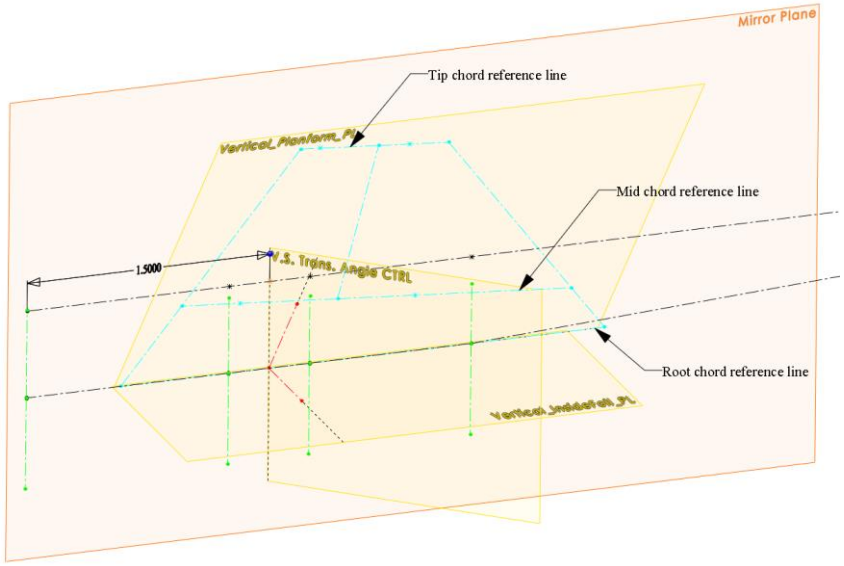

Figure 3.19: Vertical stabilizer planform reference sketches (cyan) and planes.

Each airfoil thickness control sketch is drawn on a plane coincident with their respective reference chord line (see Figure 3.19) and perpendicular to the plane that holds the planform control sketch. Thickness controls are driven by an equation set to a percentage of the corresponding sections chord length. Leading and trailing edge radii can be dimensionally constrained to match "LE Thickness" from Figure 3.11. Trapezoidal airfoils are driven by their parenting thickness control lines and the final display state is illustrated in Figure 3.20

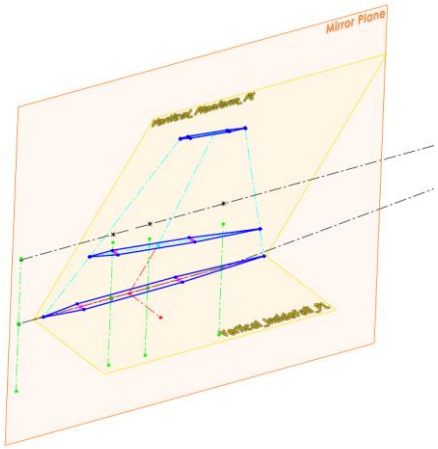

Figure 3.20: Final reference sketch display state for vertical stabilizer.

The airfoil selection is not limited to a single variety. The construction lines that define the stabilizer can be referenced by multiple airfoil types such as diamond or biconvex. More complex airfoils can also be generated on the vertical stabilizer section planes and use the planform control reference lines to drive sizing. Individually lofting each group of airfoils will create multiple solid bodies for the vertical stabilizer, all within the same aircraft configuration. Feature suppression makes it possible to deactivate the stabilizers not undergoing analysis.

Guide Curves

Before lofting sections together, guide curves can be inserted between them. This is advantageous because rather than relying on the CAD software to interpolate between sections, the loft is forced to follow each guide curve. Two conditions must be met to profit the most from lofting: 1) Each section being lofted contains the same number of line segments and 2) Traversing guide curves extend between all corresponding section nodes. If these conditions can be met, the resulting solid will be more robust and consistent between variations. To illustrate, Figure 3.21 contains a simplified rectangular-to-elliptical shape transition (REST) inlet. The upper image does not use the guide curves displayed in green, while the lower image is.

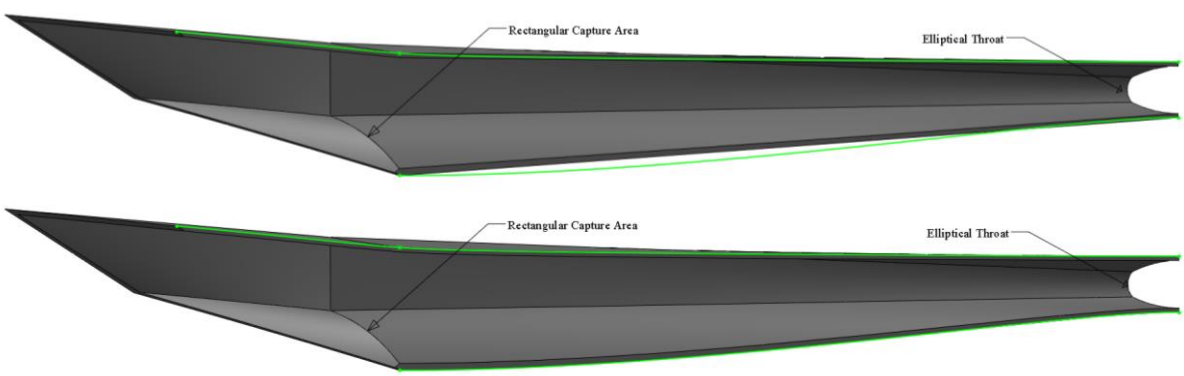

Figure 3.21: Loft without guide curves (top) and with guides (bottom).

Guide curves are particularly useful for inlet geometries generated from streamlines traced from inviscid compression fields. Such a process is commonly used when generating three-dimensional hypersonic inlets [12]. If guides are not utilized during loft processes, then the design engineer is limited to using start and end constraints or centerline parameters. Both of which do not offer the complete shape and transition control available with guide curves.

Best practices for guide curves vary on the situation and multiple guide combinations may exist that produce identical results. A majority of the guide curves used in this iMod are 3D sketches; which are simply sketches that do not require a predefined two dimensional plane and are able to freely reference objects within the three dimensional design space. This is a dynamically robust method when using straight lines from point-to-point; however, if splines are used, they should be constricted to sketch planes.

Both upper and lower center body guides are sketched on the mirror plane. The upper guide is a single spline that uses each cross sectional station as a reference point for interpolation. The lower guide curve uses straight lines for the first three ramp sections and a spline for all other downstream sections. These two guide curves are essential for consistently producing manifold geometry by forcing each section boundary all the way up to, and never beyond, the mirror plane. Guide curves which define the nose leading edge are splines generated on two separate planes – one for the upper LE radius and one for the lower LE radius. The planes are defined by three points: 1) The nose tips radius endpoint (upper or lower), 2) the first cross sections corresponding radius endpoint (upper or lower), and 3) the corresponding thickness endpoint for the first cross section. These relations enable the plane to twist along with any dihedral modifications to the outermost span section. Figure 3.22 depicts the guide curves for the mirror and wing leading edges in green. The centerline (black) and span control (cyan) sketches are shown to better represent where the guide curves are relative to the solid body (gray shaded region). Final lofting should not be performed until all guide curves are positioned.

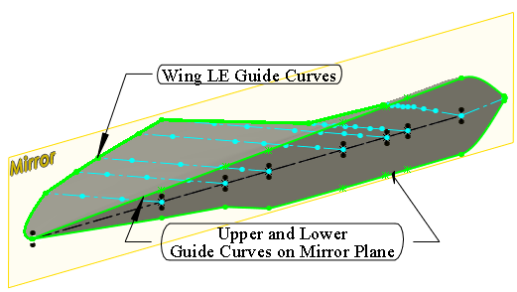

Figure 3.22: Mirror plane and wing leading edge guide curves.

All other guide curves follow what is referred to as a point-to-point approach. Meaning the guide curves reference common endpoints of each sections thickness control. Most body features and vertical stabilizer use this method. The resulting body guide curves create a web that defines the OML. Figure 3.23 displays the point-to-point guide curves for the wing and vertical stabilizer. The wing LE, upper, and lower body guides are hidden.

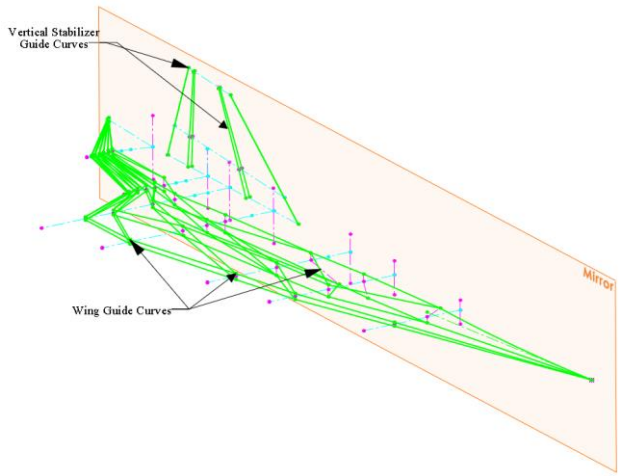

Figure 3.23: Web of point-to-point guide curves.

The same sketch color coding applies to the figure above: Magenta is for thickness control, cyan for span (chord length for vertical stabilizer), and green for guide curves

Lofting

Lofting can be performed intermittently throughout the construction process, but should only serve as a check to ensure each loft functions as intended. A minimum of two sections are required for a loft and there is no practical maximum, however, fewer sections within a loft offers more flexibility and robustness. A disadvantage of using multiple lofts chained together includes non-tangent transitions between lofts. This issue can be resolved by using common guide curves for each lofted section or by adding tangent relations between multiple curves chained together. For the BWB vehicle of this chapter, each loft section uses only two sketch profiles and tangency is enforced using guide curves. It should be noted that on rare occasions, a loft will fail to generate based on the order guide curves are selected.

Only after all control sketches are completed and guide curves are placed is lofting advisable. Reasons for this technique include: reduced clutter, avoidance of referencing solid feature vertices, the model is faster to work with (reduced load on graphics processing unit), each model update does not require complex feature regeneration, and better organization of sketch and feature hierarchy in the model (default settings will often have solid features absorb their parenting feature sketches).

Because the foundation for generating solids is now in place, lofting is as simple as selecting feature sketches and guide curves. Figure 3.24 is a snapshot from the SolidWorks environment for lofting “Body_xSection_2” and “Body_xSection_3” together to form

"Section 3". The dark green lines are selected guide curves for section three, solid cyan lines are upper and lower mirror plane guides, and the orange lines are the selected loft profiles. It is important to select "Merge Result" in the options dialogue box for a manifold geometry.

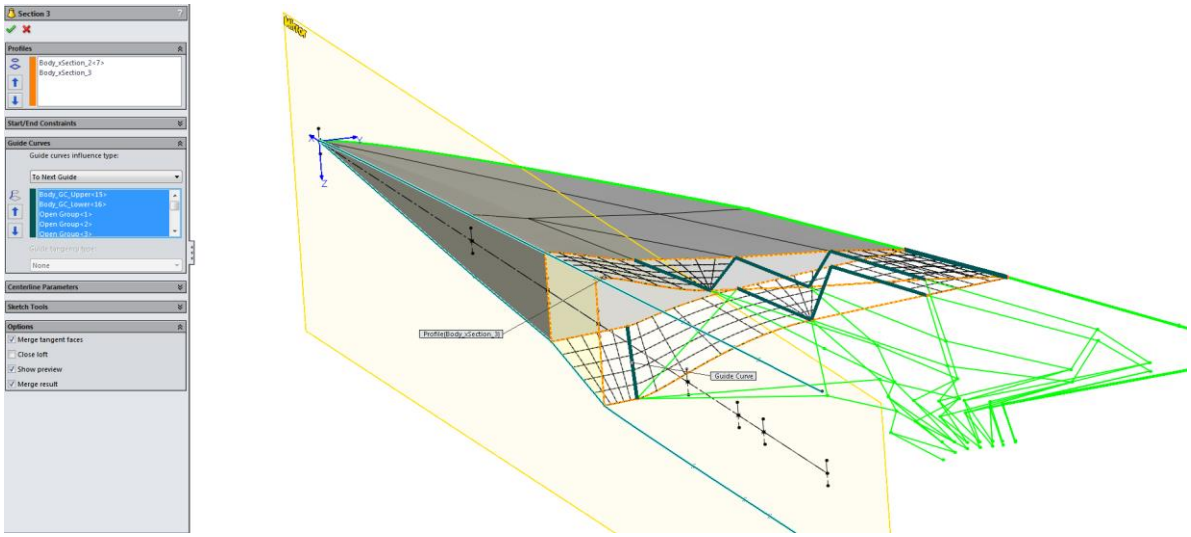

Figure 3.24: SolidWorks CAD environment for lofting between sketch profiles.

The final parameterized iMod is shown in Figure 3.25 (left). To determine capability, a robustness test is performed on the iMod (right). By producing multiple parameter combinations, failure points within the model can be identified and repaired. It is not uncommon for automatic relations to form during construction. Automatic (inferred) relations can often times be customized in the CAD software options menu. Robustness should be vigorously tested before any multidisciplinary design analysis and optimization (MDAO) is performed.

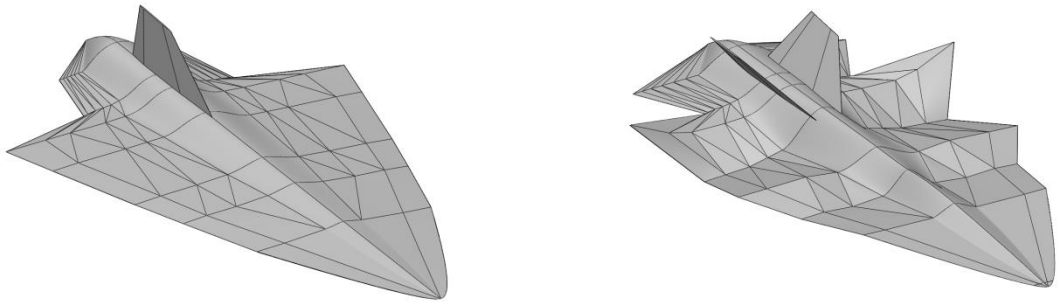

Figure 3.25: Final configuration display state (left). Robustness test (right).

3.5 Traditional Wing-Body Aircraft: Supersonic Transport

Similar to the previous BWB design, traditional wing-body aircraft can be constructed and parameterized for rapid manipulation. The methods to follow are demonstrated using a supersonic transport concept vehicle and are highly condensed. This section is intended to illustrate the capability and extensions of the iMod techniques into other classes of aircraft. These classes may include: Unmanned Aircraft Systems (UAS), commercial transports, military transports, fighter jets, and light commuter aircraft.

3.5.1 Design Parameters

Wing-body aircraft have several distinct features and cannot be effectively constructed using the point-to-pint technique from section 3.4. For a robust model, each major feature must be individually lofted. These features include the: fuselage, wing, engine pylons, engine nacelles, vertical stabilizer, horizontal stabilizer, canard or any other auxiliary parts. To capture outer mold line (OML) features of interest, the following have been selected for inclusion in the parameterized iMod.

Dihedral/Anhedral

Wing dihedral is important for aircraft lateral stability, but is selected as a metric primarily to quantify its performance impact on lift and drag.

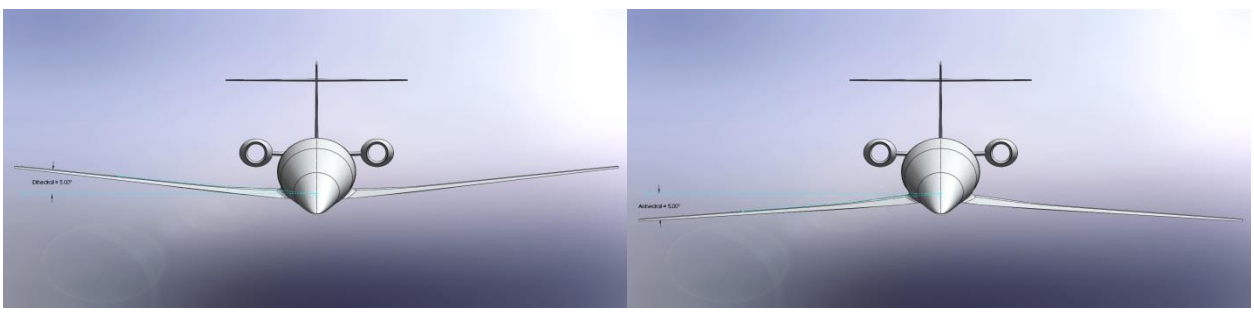

Figure 3.26: Wing dihedral set to 5° (left). Wing anhedral set to 5° (right).

Wing Span

Correlated to aspect ratio (AR) by

$$AR = \frac{b^2}{S} \qquad \text{Eq. 3.3}$$

Where b is the wing span and S is the wing area. As this parameter increases, the lift coefficient $C_{L,\alpha}$ also increases [2]. Similarly, for aircraft exceeding the speed of sound, increasing the Aspect Ratio will also increase the zero-lift drag coefficient, $C_{D,0}$.

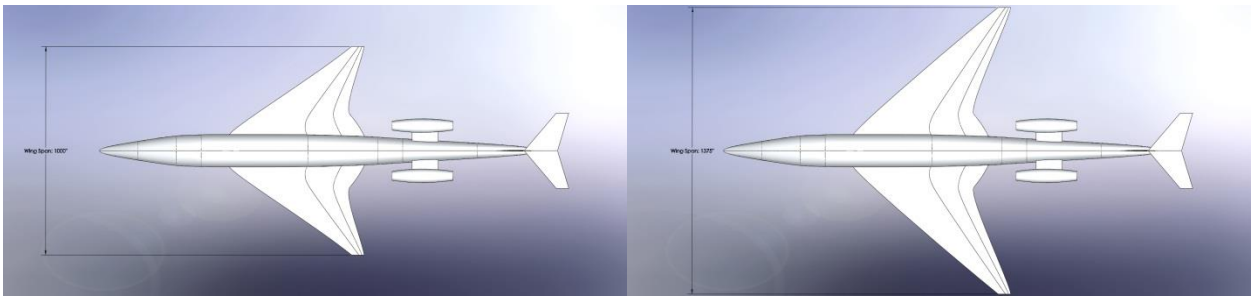

Figure 3.27: Wing span variations. b=83’ 4” (left) and b=114’ 7” (right).

Wing Thickness to Chord Ratio (t/c)

Depending on desired cruising flight flow regime (subsonic or supersonic), the wing thickness ratio will impact flight performance differently. Because smaller thickness ratios tend to increase the critical Mach number (transition speed where localized sonic flow begins to appear) supersonic aircraft will tend to have lower t/c ratios [2]. Significant disadvantages of low t/c ratios for supersonic aircraft include a reduction in fuel volume and limited structural performance.

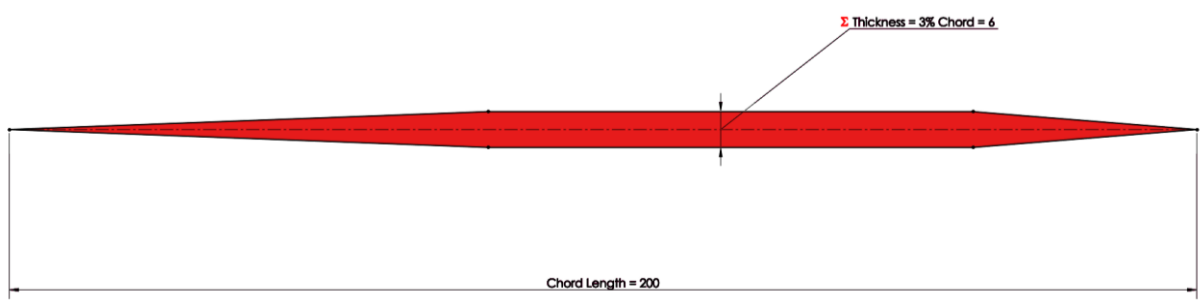

Figure 3.28: Wing t/c ratio variations.

Wing Sweep

Similar to the wing thickness ratio, wing sweep also increases the critical Mach number and decreases the zero lift drag coefficient ($C_{D,0}$) [2]. Incorporating sweep into a iMod allows engineers to analyze an array of multiple sweep angles and identify the performance tradeoffs between reducing $C_{D,0}$ (increasing sweep angle) and increasing $C_{L,max}$ (decreasing sweep angle). An additional benefit of including wing sweep as a parametric design variable is for directional stability and analyzing the impacts it has on Dutch roll.

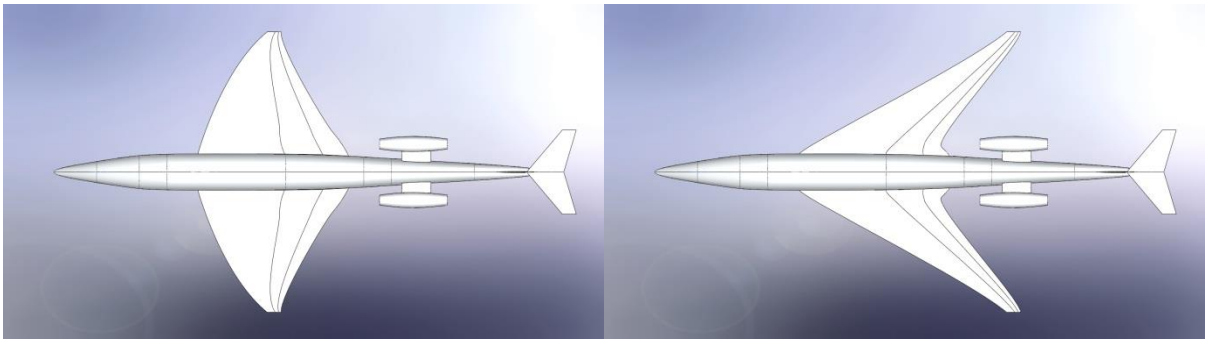

Figure 3.29: Wing sweep variations.

Stabilizer Position and Sizing

Vertical and horizontal stabilizers contribute to the lateral and longitudinal stability. Adding parametric position and sizing variations to these features will help identify locations and sizes that provide optimal control while minimizing adverse performance effects. Figure 3.30 illustrates a simple iMod reconfiguration from a single vertical and attached horizontal to a twin (dove) tail configuration.

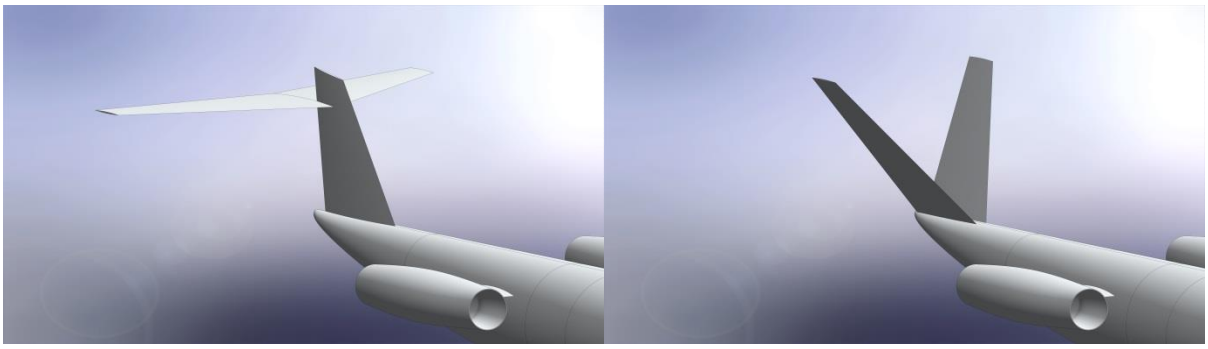

Figure 3.30: Vertical stabilizers. Single (left) and dove tail (right) configurations.

This process, when done manually, takes an engineer less than 5 minutes. Two simple steps are required: suppress the horizontal stabilizer and then increase the angle value with respect to the XZ plane (stability coordinate system) of the vertical stabilizer. Two stabilizing features are created when the solid body is mirrored over the XZ plane.

Control Surfaces

Major design considerations for control surfaces include: position, sizing, and deflection angle. Including the capability to control these parameters enables a rapid

succession of optimization cycles to determine candidate configurations providing maximum trim effectiveness while minimizing adverse effects such as drag.

After the aerodynamic forces and static margin are determined (see section 4.2.2), parameters such as sizing and deflection angles can be incorporated into the iMod. To reduce computational resources, control surface analyses should only be considered in the latter stages of the initial design cycles. Including a trimmed aircraft configuration in the initial design analysis may expose significant aerodynamic and structural issues early on – avoiding costly and time consuming design changes later on.

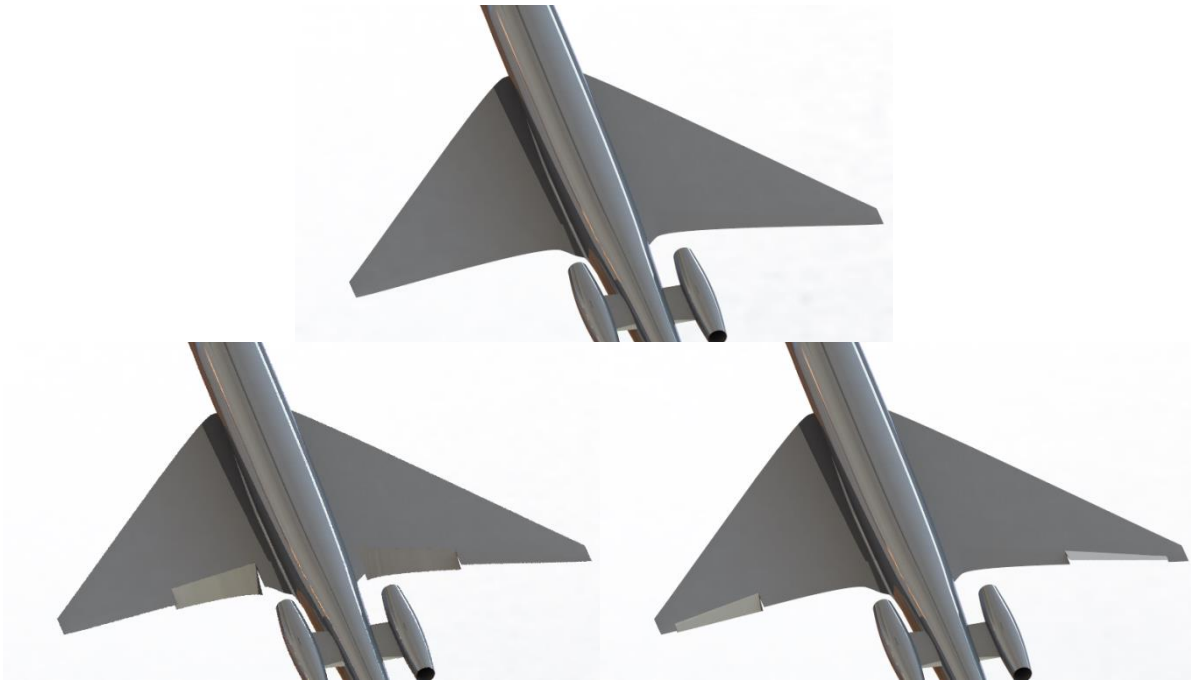

Figure 3.31: Control surface deflections.

The upper image of Figure 3.31 is the default zero degree deflection state. The image in the lower left corner has 20 degree flap deflections. The lower right image has 15 degree aileron deflections for a positive roll (right) maneuver.

3.5.2 Summary of Construction Process

Constructing traditional style aircraft takes place in three basic stages: 1) Fuselage, 2) Wing, and 3) Auxiliary components. Auxiliary components include stabilizers, engine pylons, engine nacelles, canards, winglets, and other components deemed appropriate by the engineering design team. Each stage follows the underlying construction technique previously shown in the *Simple Parametric Example* of section 3.2.2 – obeying the three step

process: construction lines, feature sketches, and then lofting. It is important to complete all sketches for each feature and then begin lofting in the proper order of dependency. This will improve efficiency and reduce undesired references. Dependency orders can vary, but as a general rule, it is best to loft the root feature before any others. For an aircraft this is the fuselage. Without a main adjoining feature the wing and tail stabilizers are separate bodies and detached until the fuselage is created to unite them. Lofting can be thought of as a growing process where features are extensions from their larger counterparts. If lofting follows the order: fuselage, wing, winglet, vertical stabilizer, and then horizontal stabilizer (for a T-tail configuration) while optioning to unite each feature as it is created; there is only a single solid body throughout the entire process.

CHAPTER 4. SIMULATION BASED DESIGN METHODOLOGY

The method used to demonstrate the robustness and flexibility of iMods incorporates physics simulations and data post processing techniques to evaluate each parametric variation. In particular, CFD (STAR-CCM+) is used to evaluate the forces and moments on the aircraft and a MatLab code evaluates the performance. Performance scoring and criteria are covered at greater length in Section 4.2.4. The basic process is illustrated in Figure 4.1 and begins with mission requirements setting the design targets. After targets are set, initial design models are created. The initial designs are simply concept models that represent the class or classes of aircraft which best suit the mission requirements. These concept models also determine the initial aircraft scaling, such as total length and wing span. After the initial design(s) are generated, iMods are developed and the process becomes cyclic. The first iMod in the design cycle will be known as the "baseline" design, as this model sets the standard from which all other variations are measured from. CFD physics simulations generate raw data that is gathered and analyzed for performance by a data post processing MatLab code which scores the design based on how well it meets the targets.

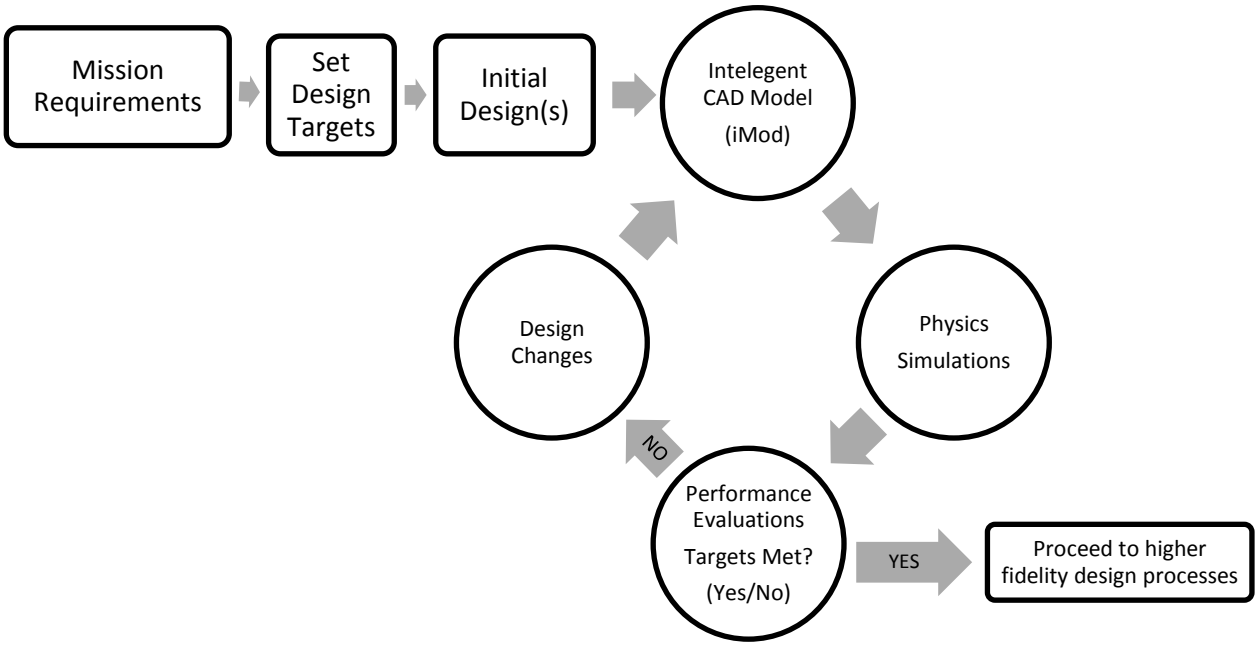

Figure 4.1: Simulation based design process flow chart.

If performance evaluations reveal the vehicle configuration does not meet requirements, its parameters are modified by design engineers or updated using an optimization routine, and the cycle continues. Once a feasible design is found, it proceeds to the next design phase and higher fidelity analyses are conducted. Analysis may include a full 3-dimensional stability CFD modeling to determine all forces and moments in pitch, roll, yaw, and coupled rotations or structural modeling within a finite element analysis (FEA) code.

4.1 Physics Simulation Setup (CFD)

The primary analysis tool for the case study in CHAPTER 5 is STAR-CCM+ Version 8.06.005. This commercially available CFD software is capable of simulating multi-million cell meshes for full three-dimensional geometries. The setup consists of six basic categories: 1) Geometry. Which includes importing the CAD model, naming, and creating the domain, 2) Physics continua and solvers, 3) Mesh continua, 4) Boundary conditions, 5) Setting up free stream flow characteristics, and 6) Adding reports to monitor force and moment data. These six setup steps are briefly outlined in the following sections.

4.1.1 Geometry

Several file types can be imported into STAR-CCM+. For CFD simulations, only solid body types are used to avoid otherwise time consuming processes associated with surface models – such as surface stitching and wrapping. Both Parasolid and STEP files are used for the case study in CHAPTER 5. STEP files are convenient if the CAD modeling software allows exporting of both solid and surface geometry. This enables the naming of solid body surfaces within the CAD software and eliminates the process within the CFD software. Naming the surfaces within an iMod also preserves conventions within all model variations and configurations (provided surfaces are not created or eliminated). Additionally, some CAD software packages have the capability to attach non-physical attributes which would assign proper boundary conditions, mesh properties, etc. to the solid surfaces.

The created air domain is solid sphere (or hemisphere for symmetrical half body simulations) surrounding the CAD model. The free stream domain is sized based on the scale of model. For simulations at supersonic and hypersonic velocities, the distance between the nose of the aircraft and the outer boundary of the free steam can be on the order of 1/2 to 1/4 the overall vehicle length. For the best accuracy, a minimum distance of 8-10 times the overall length behind the aircraft should be used [13]; however, distances of three times the overall vehicle length are sufficient for supersonic and hypersonic simulations.

Under subsonic conditions, information is able to travel upstream and larger domains (both upstream and downstream) must be considered. Simulations that include propulsion analysis should also have an appropriately sized domain to capture the entire exhaust plume. The free stream is elongated as shown below in Figure 4.2. The upper half of the dark gray profile is revolved 180 degrees around the x-axis to form a solid axisymmetric half body domain.

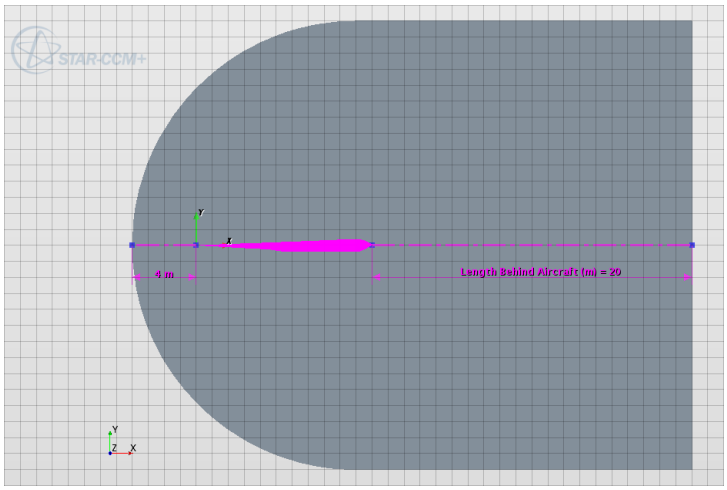

Figure 4.2: Profile used for free stream air domain.

4.1.2 Physics Continua

For the CAD-centric design methodology, each engineering discipline is in charge of their respective area(s) of expertise. These specialty associations are vital to achieve as high of accuracy as possible when simulating physical conditions and environments. Results from CFD codes and software can significantly vary based on solver settings; therefore, an immense amount of subject knowledge is required to properly setup an analysis. For the investigations throughout this paper, a template created using CD-Adapco's best practices is implemented to ensure accurate solutions. A summary of the selected physics models are briefly described below.

For strictly analyzing the outer mold line in transonic, supersonic, and hypersonic flows, full three-dimensional steady state solutions are found using Reynolds-Averaged Navier-Stokes equations. The coupled flow and energy models incorporate the AUSM+ (advection upstream splitting method) scheme to more accurately capture the shock and contact discontinuities [14]. The ideal gas law is used express the air density as a function of the temperature and pressure. Turbulence is modeled using the SST (shear-stress transport) K-Omega technique by Menter [15] with an all y+ wall treatment.

4.1.3 Mesh Continua

The mesh continua used in this study includes two main categories: models and reference values. Mesh models set the cell types and quality. Reference values dictate the properties of added mesh models. Value categories vary depending on the mesh models used in a simulation.

Models

For the supersonic and hypersonic external aerodynamic applications, polyhedral meshes have proven to perform well [13]. A prism layer mesh should also be used to capture the boundary layer. A surface remesher is also used to improve the imported CAD models initial surface quality and optimize it for volume meshing. The illustration below in Figure 4.3 shows an example of an initial geometry surface (left) and the remeshed surface (right). The substantial quality increase is valuable for analyzing the performance of leading edges under supersonic and hypersonic flight conditions. It is not unusual for a hypersonic aircraft to have a LE radius between .03 and .05 inches [16]. Because of these small features, special care must be taken to capture the designed geometry to improve simulation accuracy.

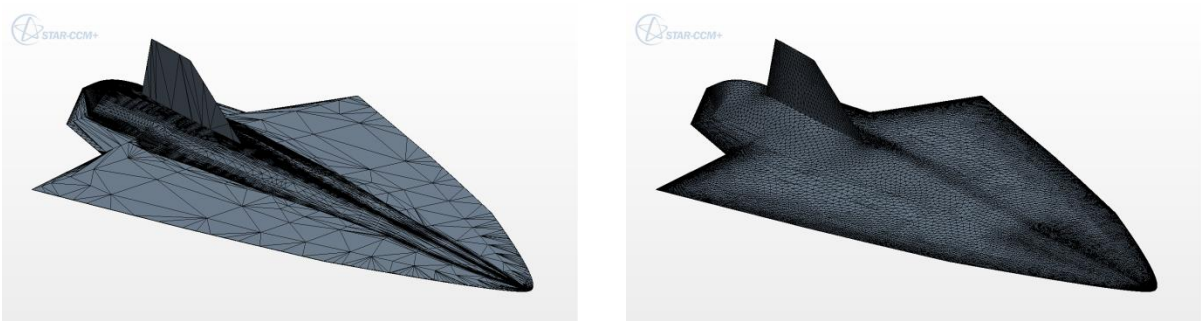

Figure 4.3: Initial geometry and remeshed surface comparison.

Reference Values

Polyhedral, prism, and surface remesher models include the following major reference values: Base size, prism layer control parameters, surface cell controls, and volumetric cell controls. To efficiently simulate geometries, each specified boundary region in the domain should specify custom mesh conditions. The free stream and symmetry boundaries should have equal sizing constraints and the far field cells may be sized on the order of the overall body length.

The base size can be used to facilitate mesh refinement on a global scale by setting cell boundary sizes to a percentage of the base size. Doing this enables changes by altering a single parameter rather than to all boundary parameters.

Prism layer controls include the number of prism layers, prism layer stretching, and the total thickness for the prismatic cell layers. The prism layer stretching ratio specifies the thickness of each cell relative to the previous cell layer. Stretching ratio is important for controlling wall Y+ values. Wall Y+ indicates how well the mesh is able to resolve the boundary layer and accurately model turbulence.

Surface cell controls may include: growth rate, curvature, minimum size, and target size. Surface growth rate is a ratio which represents the maximum size difference between the edges of adjacent cells. This property is important for maintaining smooth transitions across regions with dissimilar mesh refinement settings. Curvature dictates cell face sizes on a curve based on arch length using an operator defined quantity of points around an equivalently sized circles circumference. The minimum and target sizes can be defined as percentages of the base cell size or as absolute values. Boundaries which require mesh refinements can be dramatically impacted by these two values. Minimum size restrictions regulate the surface mesher by preventing small geometric features from becoming too refined. Target size sets the preferred surface cell dimensions and facilitates cell size optimization by allowing slight deviations above and below the specified target value.

The volumetric mesh domain is indirectly sized by surface cell controls. After the first cell layer is generated on the surface, volumetric controls take over. Polyhedral meshes in STAR-CCM+ have two defining properties – density and growth factor. The density factor either increases for values greater than 1.0 or decreases for values less than 1.0. By increasing the density above 1.0, the mesh domains cell count will also increase. The opposite holds for reducing the value below 1.0. Polyhedral growth factors determine the rate at which the cell volumes grow between boundaries with fine mesh settings to those with coarser settings.

4.1.4 Boundary Conditions

Simulations can be analyzed based on two primary stability conditions. Longitudinal (pitch) stability analyses only requires half body symmetrical simulations while lateral (roll) and directional (yaw) stability require full body simulations. Figure 4.4 presents the two simulation types.

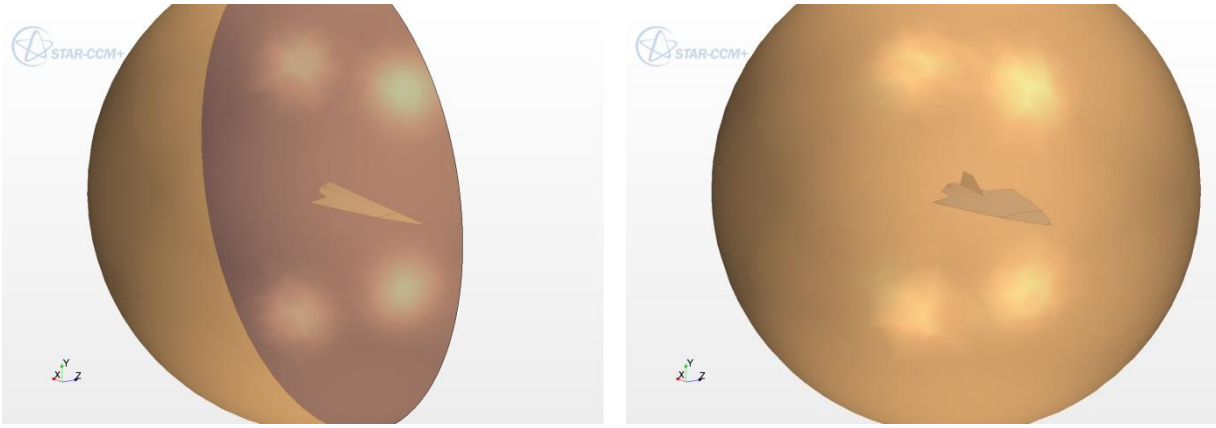

Figure 4.4. Half (left) and full (right) body simulation boundary conditions.

For pitch simulations, only half the domain is necessary. A symmetrical boundary condition is applied to the mirror plane. This boundary is represented in the left image of Figure 4.4 as a dark blue region. Both half body (left image) and full body (right image) simulations use free stream boundary conditions (gold region) for the air domain and wall boundary conditions (grey region) for the aircraft OML.

4.1.5 Force and Moment Reports

Reports in STAR-CCM+ are used to monitor physical properties by extracting the desired information from the applied physics models within the simulation. Multiple reports are available in STAR-CCM+, ranging from mass flow rates to heat transfer properties and user defined expressions. For the purposes of this analysis, force and moment reports are selected. Full body aerodynamic forces and moments are the primary reports used for evaluating performance; however, the body may be split into smaller components. Breaking down the aircraft into sections is useful when determining the impact of specific parametric changes. For instance, if an aircraft forebody is altered and all other parameters remain constant, the impact of that change can be seen on each individual component. Other examples include stabilizer contributions to restoring moments. When partitioning the aircraft, it is important to ensure the reference pressure is taken into consideration.

Symmetrical simulations with pitch only maneuvers require lift, drag, and pitching moment reports because it is assumed that all other body forces cancel with their symmetrical counterparts. Full body simulations involving roll and yaw maneuvers require force and moment values associated with each of the three Cartesian component directions. Sign convention is derived using the standard stability coordinate system shown in Figure 4.5. A positive pitching moment (M_y) is nose up. Positive yawing moment (M_z) is to the nose right

and a positive roll moment (M_x) is right wing down when viewing the aircraft from behind in the positive x-direction.

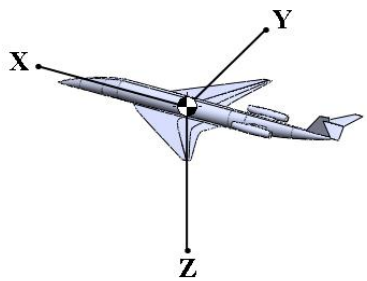

Figure 4.5: Standard body fixed stability coordinate system.

Exporting report data for post processing is done with the use of .csv files. In STAR-CCM+, the files are exported as data points from monitor plots. Monitors are set to capture the data points when the simulation is converged by using iteration triggers. These triggers are set to extract the values from the desired reports at specified iterations. Consistent data formatting of rows and columns is important when using a code or script to process the data.

4.2 Performance Evaluations

Data is gathered from the CFD force and moment reports in the form of *.csv files. Each report file is read into MatLab where the raw data is transformed using the free stream flow characteristics data table, and a performance index value is assigned based on the set design requirements. For the case study in CHAPTER 5, the primary performance metrics include; lift to drag ratio (L/D) translated into range, static stability, and total volume within the vehicles OML. These basic vehicle performance parameters are discussed below.

4.2.1 L/D

The ratio of lift to drag is a very important metric in determining overall aircraft performance. It is a measure of efficiency and has a linear relationship with range through the Breguet range equation [Eq. 4.1]. It should be noted that this equation assumes steady level flight conditions where Thrust = Drag and Lift = Weight. Also, L/D and TSFC remain constant. To effectively utilize the Breguet range equation, the flight trajectory can be divided into smaller segments and approximated as steady and level.

$$R = \frac{L}{D}\frac{V}{TSFC} ln\left(\frac{W_i}{W_f}\right) \qquad \text{Eq. 4.1}$$

Where R is the range, L is lift, D is drag, V is velocity, TSFC is the thrust specific fuel consumption, W_i is the initial weight, and W_f is the final weight. It is also be appropriate to write the Breguet range equation in terms of specific impulse (I_{sp}). This is shown in equation Eq. 4.2.

$$R = V\frac{L}{D} I_{sp} ln\left(\frac{W_i}{W_f}\right) \qquad \text{Eq. 4.2}$$

Because of the significant performance impact, L/D contributes substantially to the overall performance index for the case study in CHAPTER 5.

4.2.2 Static Stability

Aerodynamic data is extracted from CFD results for the full aircraft. Forces and moments are set to report about the nose (origin) and later transformed to a range of locations along the aircrafts X and Z axes using a post processing script written in MatLab. The standard stability coordinate system from Section 4.1.5 is used. First, rotations are computed from the user defined freestream table, force vectors, moment vectors, and the Eulerian transformation matrices. The Euler transformations [17] follow a sequence of three rotations: 1) Yaw, 2) Pitch, and 3) Roll and are shown in equations Eq. 4.3, Eq. 4.4, and Eq. 4.5. For convenience, the notations from Table 4.1 are implemented:

Table 4.1: Abbreviations used in Eulerian transformation matrices.

Yaw Angles	**Pitch Angles**	**Roll Angles**
$C\beta = \cos(\beta)$	$C\alpha = \cos(\alpha)$	$C\psi = \cos(\psi)$
$S\beta = \sin(\beta)$	$S\alpha = \sin(\alpha)$	$S\psi = \sin(\psi)$

1) Yaw

$$\begin{Bmatrix} x_1 \\ y_1 \\ z_1 \end{Bmatrix} = \begin{bmatrix} C\beta & S\beta & 0 \\ -S\beta & C\beta & 0 \\ 0 & 0 & 1 \end{bmatrix} \begin{Bmatrix} x_0 \\ y_0 \\ z_0 \end{Bmatrix} \qquad \text{Eq. 4.3}$$

2) Pitch

$$\begin{Bmatrix} x_2 \\ y_2 \\ z_2 \end{Bmatrix} = \begin{bmatrix} C\alpha & 0 & -S\alpha \\ 0 & 0 & 0 \\ S\alpha & 0 & C\alpha \end{bmatrix} \begin{Bmatrix} x_1 \\ y_1 \\ z_1 \end{Bmatrix} \qquad \text{Eq. 4.4}$$

3) Roll

$$\begin{Bmatrix} x_3 \\ y_3 \\ z_3 \end{Bmatrix} = \begin{bmatrix} 1 & 0 & 0 \\ 0 & C\psi & S\psi \\ 0 & -S\psi & C\psi \end{bmatrix} \begin{Bmatrix} x_2 \\ y_2 \\ z_2 \end{Bmatrix} \qquad \text{Eq. 4.5}$$

The vector $< x_0, y_0, z_0 >$ represents the original force or moment vector aligned with the XYZ body fixed coordinate system and $< x_3, y_3, z_3 >$ is the final vector orientation aligned with the wind. Once the rotations are applied to the force and moment vectors, they are translated to the volumetric C_g (center of gravity). This provides an approximate starting location for applying small (approx. 1% the total length) variations to the C_g's position. By doing this, a range of suitable locations is determined for positive static stability. Because a majority of the simulations are symmetrical for the case study in CHAPTER 5, they do not include yaw and roll; therefore longitudinal static stability is used as the primary performance metric. To quantify the longitudinal static stability; static margin [18] is defined as the distance between the center of gravity and the neutral point (np) divided by the mean chord length. Eq. 4.6 represents this property. Positive values indicate the center of gravity (COG) is forward relative to the neutral point and has a pitch down restoring moment. This positive positional relationship for np and C_g defines a statically stable aircraft.

$$S.M. = \frac{l_{np}}{\bar{c}} \qquad \text{Eq. 4.6}$$

Where l_{np} is the longitudinal distance measured from the COG to the neutral point and $\bar{c}$ is the mean wing chord length. For BWB aircraft, the entire planform is considered the wing. The neutral point is defined as the location where the total pitching moment does not change with small perturbations in angle of attack. If the COG is located at this point, the aircraft is neutrally stable.

It should also be noted that STAR-CCM+ is capable simulating geometries with 6 degrees of freedom when provided with the mass moments of inertia. This aids in determining dynamic stability performance and may be considered when proceeding to higher fidelity design analyses.

4.2.3 Total Volume

Aircraft volume is an essential metric for determining overall performance. The target volume is set by estimating the space required to contain all essential aircraft components for a successful mission. These components include but are not limited to; payload and cargo, structure, fuel, electronics and avionics, hydraulics, and propulsion subsystems (fuel system, air induction system, engine controls, etc.). Of these, the three most prominent components for volume considerations are fuel, payload, and structure.

Given mission range requirements, an approximate fuel volume can be determined based on current engine performance data. Payload volume is also set by mission requirements. Because there is no direct way to determine the percentage of overall volume required for a structurally sound aircraft other techniques must be used. Approximations can be made based on legacy aircraft, however, adding FEA as an additional physics simulation to the previous design stage can be advantageous. Adding a structural design group within the simulation based design process allows early identification of structurally problematic regions within the OML. Once identified, the volume can be expanded to allow for larger structural members where the current material has exceeded its yield strength.

4.2.4 Scoring Performance Metrics

As the design process progresses through iterations, it is important to track how each change impacts the vehicle. Each design variation is evaluated based on how well the performance metrics accomplish the requirements from three categories provided in section 2.3.1. This can be a very complex process and involves input from all design disciplines. For the purposes of this study, each metric drives vehicle performance primarily based on range and stability. L/D may be considered to be the most important factor as it contributes greatly to the overall range of the vehicle. Total aircraft volume can also be used in conjunction with L/D to improve range estimations. Due to insufficient definition for system and subsystem sizing and placement during the conceptual design stages, the impact total volume has on the overall vehicle is unknown. Static stability is determined based on static margin. A positive static margin is considered stable. If the design variation exceeds 4% it is considered viable. A negative static margin is considered unstable and requires advanced flight control systems. If an aircraft scores high for all other performance metrics but fails to meet stability requirements, the design can be looked at in closer detail for potential solutions to correct the instability. This scoring process provides engineers quick and consistent methods for determining changes for subsequent design iterations and aids in tracking convergence toward each individual requirement.

4.3 Design Changes

After performance is evaluated and the design fails to meet mission targets, modifications must be implemented. Two design update methods outlined below include trade studies and optimization schema.

4.3.1 Trade Studies

Trade studies involve engineering human interaction to determine the most optimal design. This system engineering method requires the engineer to make conscious tradeoffs and weight conflicting benefits [19]. Because of human interaction, trade studies are both advantageous and detrimental to the design process. A major advantage includes allowing a knowledgeable engineer to make methodical changes to determine which design variables drive the performance closer to and further from the targets. The primary disadvantage of this process is the increased time to cycle through design variations due to dependence on human interaction. Trade studies may provide satisfactory results in fewer cycle iterations - making them ideal when computational resources are limited.

4.3.2 Optimization Schema

If computational resources are not an issue, there are many multidisciplinary optimization schemes available. Due to the nature of this particular design challenge, many gradient based optimization schemes are impractical as the performance results are highly dependent the mesh refinement. This causes difficulty when determining if an increase or decrease in a performance metric is caused by the small perturbation of a design variable or by a change in the cell architecture of the mesh domain. Optimization methods must be capable of capturing an enormous number of design variables and converging on multiple solutions due to the large number of dimensions that drive an iMod. Particle swarm optimization schemes with elements of value driven design have proven useful for handling the enormous amounts of data associated with analyzing aircraft OML features.

CHAPTER 5. CASE STUDY

This study illustrates a single iteration through a simulation based design process for the outer mold line of a hypersonic aircraft. Mission requirements are provided from the customer and design targets are set. An initial concept model classification is defined to correspond with the mission goals design targets. Next, the initial concept model is dimensioned and design variables for iMod parameterization resolved. Flow and energy physics are simulated using CFD and performance evaluations conducted. The final stage of the iteration process is included in the chapter to follow and discusses potential methods for design changes.

5.1 Requirements

The following list of requirements is created for a high speed flight demonstration research vehicle with the capability to extend into military applications.

- L/D > 6.5
- Airframe integrated scramjet engine.
- Cruise range over 5000 nautical miles (nm).
- Non-recoverable. Controlled crash into Pacific Ocean.
- 10,000 lb. GTOW with 4,000 lb. fuel capacity

5.2 Design Targets

To address high speed flight, all variations are simulated using CFD in an environment replicating Mach 6 cruise at approximately 103,000 feet (31,000 m). To maximize cruise range, the model is assumed to begin flight at 30,000 feet after deploying from the wing of a B-52. In order to bring the aircraft up to supersonic speeds required for scramjet operation, a rocket booster is used. Because the aircraft is a demonstration research vehicle, only the flight data needs recovering and there is no need for complex landing systems.

5.3 Initial Concept Model

The requirement for an airframe integrated scramjet engine is fulfilled by housing the inlet on the underside of the aircraft and nozzle out the rear. An initial concept model capable of characterizing these properties and also offers high volumetric capability is a blended wing body aircraft with a length scale of 10 meters. As stated in section 3.1, this value is

based on legacy aircraft similar to NASA's X-43. Figure 5.1 illustrates the initial blended wing body conceptual model. This model represents the historical conceptual pencil and paper sketches used to estimate aerodynamics and weights by comparing to legacy designs. However, it is now a digital representation which can be imported into a CFD code and simulated to provide more accurate first-order sizing.

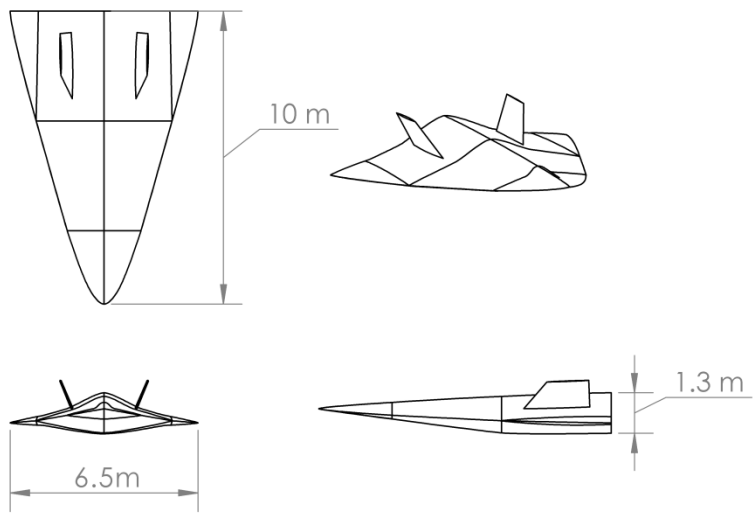

Figure 5.1: Initial hypersonic wave rider concept model.

5.4 iMod

The 10 meter iMod constructed in section 3.4.2 is used for this analysis. Selected design parameters are included in Table 5.1. Each batch has seven variations for a total of 56 model configurations. The extent of design variable modification varies throughout the batch. For example, "Batch 1" modifies the iMods longitudinal body section angles with respect to the centerline. The first variation changes the angle of only the last loft section (section 7). The second variation retains the first and also adjusts the angle for section 6. The trend continues through to variation 7 where all body section angles are different than the unmodified (baseline) configuration.

Table 5.1: Test parameters.

Batch	Variation Range	Parameters Modified
1	PS01_V01 – PS01_V07	Body Section Angles
2	PS01_V08 – PS01_V14	Centerline body cross section thicknesses
3	PS01_V15 – PS01_V21	Wing Dihedral

Table 5.2 continued

4	PS01_V22 – PS01_V28	Wing Span
5	PS01_V29 – PS01_V35	Wing Span
6	PS01_V36 – PS01_V42	Wing Span
7	PS01_V43 – PS01_V49	Wing Thickness
8	PS01_V50 – PS01_V56	Wing LE Thickness

Each set of selected design parameters are formulated in what SolidWorks refers to as a "Design Table". Design tables are organized using an Excel Spreadsheet with dimension names across the top row and model configuration names in the first column. The inner matrix of numbers assigns each configuration a corresponding dimensional value. Figure 5.2 is an example design setup. Batches 1, 2, and 3 are color coded in the first column as varying shades of gray. The row shaded in red is the baseline (default) configuration; the dimensions of this row are never changed. Orange cells in the central matrix highlight altered dimensions within each variation. Color coding is optional, but makes reading the spread sheet much simpler. Formatting is software dependent. SolidWorks uses the top left most cell to reference a the part file to which it is linked and only allows non-dimensional cells three rows below the last model variation. Dimension descriptions are located below this threshold and also serve as convenient cells for equations and logic statements.

Design Table for: HARPc_PS01_VDT_Batch_1-2-3

	D7@Center Line_Body CNTRL	D100@Center Line_Body CNTRL	D200@Center Line_Body CNTRL	D300@Center Line_Body CNTRL	D400@Center Line_Body CNTRL	D500@Center Line_Body CNTRL	D600@Center Line_Body CNTRL	D700@Center Line_Body CNTRL	D1@xSectionThick_CNTRL	D2@xSectionThick_CNTRL	D3@xSectionThick_CNTRL	D4@xSectionThick_CNTRL	D5@xSectionThick_CNTRL	D6@xSectionThick_CNTRL	D7@xSectionThick_CNTRL	D10@xSectionThick_CNTRL	D30@xSectionThick_CNTRL	D20@xSection
Baseline	10.0000	90.0000	90.0000	90.0000	90.0000	90.0000	90.0000	90.0000	0.1200	0.1760	0.2150	0.2850	0.3290	0.3500	0.4000	0.1760	0.4000	0.4000	0.412
PS01_V01	10.0000	90.0000	90.0000	90.0000	90.0000	90.0000	90.0000	90.0000	0.1200	0.1760	0.2150	0.2850	0.3290	0.3500	0.4000	0.1760	0.4000	0.4000	0.412
PS01_V02	10.0000	90.0000	90.0000	90.0000	90.0000	90.0000	90.0000	92.0000	0.1200	0.1760	0.2150	0.2850	0.3290	0.3500	0.4000	0.1760	0.4000	0.4000	0.412
PS01_V03	10.0000	90.0000	90.0000	90.0000	90.0000	90.0000	92.0000	90.0000	0.1200	0.1760	0.2150	0.2850	0.3290	0.3500	0.4000	0.1760	0.4000	0.4000	0.412
PS01_V04	10.0000	90.0000	90.0000	90.0000	90.0000	92.0000	90.0000	90.0000	0.1200	0.1760	0.2150	0.2850	0.3290	0.3500	0.4000	0.1760	0.4000	0.4000	0.412
PS01_V05	10.0000	90.0000	90.0000	90.0000	92.0000	90.0000	90.0000	90.0000	0.1200	0.1760	0.2150	0.2850	0.3290	0.3500	0.4000	0.1760	0.4000	0.4000	0.412
PS01_V06	10.0000	90.0000	90.0000	92.0000	90.0000	90.0000	90.0000	90.0000	0.1200	0.1760	0.2150	0.2850	0.3290	0.3500	0.4000	0.1760	0.4000	0.4000	0.412
PS01_V07	10.0000	90.0000	92.0000	90.0000	90.0000	90.0000	90.0000	90.0000	0.1200	0.1760	0.2150	0.2850	0.3290	0.3500	0.4000	0.1760	0.4000	0.4000	0.412
PS01_V08	10.0000	90.0000	90.0000	90.0000	91.0000	92.0000	93.0000	93.0000	0.1200	0.1760	0.2150	0.2850	0.3290	0.3500	0.4000	0.1760	0.4000	0.4000	0.412
PS01_V09	10.0000	90.0000	90.0000	90.0000	90.0000	90.0000	90.0000	90.0000	0.1200	0.1760	0.2150	0.2850	0.3290	0.3500	0.5000	0.1760	0.4000	0.4000	0.412
PS01_V10	10.0000	90.0000	90.0000	90.0000	90.0000	90.0000	90.0000	90.0000	0.1200	0.1760	0.2150	0.2850	0.3290	0.4500	0.5000	0.1760	0.4000	0.4000	0.412
PS01_V11	10.0000	90.0000	90.0000	90.0000	90.0000	90.0000	90.0000	90.0000	0.1200	0.1760	0.2150	0.2850	0.4290	0.4500	0.5000	0.1760	0.4000	0.4000	0.412
PS01_V12	10.0000	90.0000	90.0000	90.0000	90.0000	90.0000	90.0000	90.0000	0.1200	0.1760	0.2150	0.3850	0.4290	0.4500	0.5000	0.1760	0.4000	0.3000	0.512
PS01_V13	10.0000	90.0000	90.0000	90.0000	90.0000	90.0000	90.0000	90.0000	0.1200	0.1760	0.3150	0.3850	0.4290	0.4500	0.5000	0.1760	0.4000	0.3000	0.512
PS01_V14	10.0000	90.0000	90.0000	90.0000	90.0000	90.0000	90.0000	90.0000	0.1200	0.2670	0.3150	0.3850	0.4290	0.4500	0.5000	0.1760	0.4000	0.3000	0.512
PS01_V15	10.0000	90.0000	90.0000	90.0000	90.0000	90.0000	90.0000	90.0000	0.2200	0.2670	0.3150	0.3850	0.4290	0.4500	0.5000	0.2760	0.4000	0.3000	0.512
PS01_V16	10.0000	90.0000	90.0000	90.0000	90.0000	90.0000	90.0000	90.0000	0.1200	0.1760	0.2150	0.2850	0.3290	0.3500	0.4000	0.1760	0.4000	0.4000	0.412
PS01_V17	10.0000	90.0000	90.0000	90.0000	90.0000	90.0000	90.0000	90.0000	0.1200	0.1760	0.2150	0.2850	0.3290	0.3500	0.4000	0.1760	0.4000	0.4000	0.412
PS01_V18	10.0000	90.0000	90.0000	90.0000	90.0000	90.0000	90.0000	90.0000	0.1200	0.1760	0.2150	0.2850	0.3290	0.3500	0.4000	0.1760	0.4000	0.4000	0.412
PS01_V19	10.0000	90.0000	90.0000	90.0000	90.0000	90.0000	90.0000	90.0000	0.1200	0.1760	0.2150	0.2850	0.3290	0.3500	0.4000	0.1760	0.4000	0.4000	0.412
PS01_V20	10.0000	90.0000	90.0000	90.0000	90.0000	90.0000	90.0000	90.0000	0.1200	0.1760	0.2150	0.2850	0.3290	0.3500	0.4000	0.1760	0.4000	0.4000	0.412
PS01_V21	10.0000	90.0000	90.0000	90.0000	90.0000	90.0000	90.0000	90.0000	0.1200	0.1760	0.2150	0.2850	0.3290	0.3500	0.4000	0.1760	0.4000	0.4000	0.412
Dimension Discription	**Total Length**	**Body Section Angles wrt Vertical (-Z axis)**							**UPPER BODY: xSection Heights**							**LOWER BODY: xSe**			

Figure 5.2: Example of a design table (segment from batches 1, 2, and 3).

Design tables extend beyond the capability to execute quick multi-dimensional modifications in a single spreadsheet; they reveal opportunity for automated optimization. Discussion on methods for design modification is included in section 4.3.2.

5.5 Physics Simulations

STAR-CCM+ (version 8.06.005) from CD-Adapco is used to perform CFD flow and energy physics. An automated batch process imports *.STEP AP203 formatted CAD files. Using this file type is beneficial because feature names can be appended to faces of the solid model and transferred into CFD. All iMod configurations retain naming conventions from the original model – eliminating the need to name every surface for each variant within the CFD software. Boundary conditions and mesh sizing are also automatically assigned based on face naming conventions. Figure 5.3 illustrates the how the iMod is broken down into features of interest for CFD analysis.

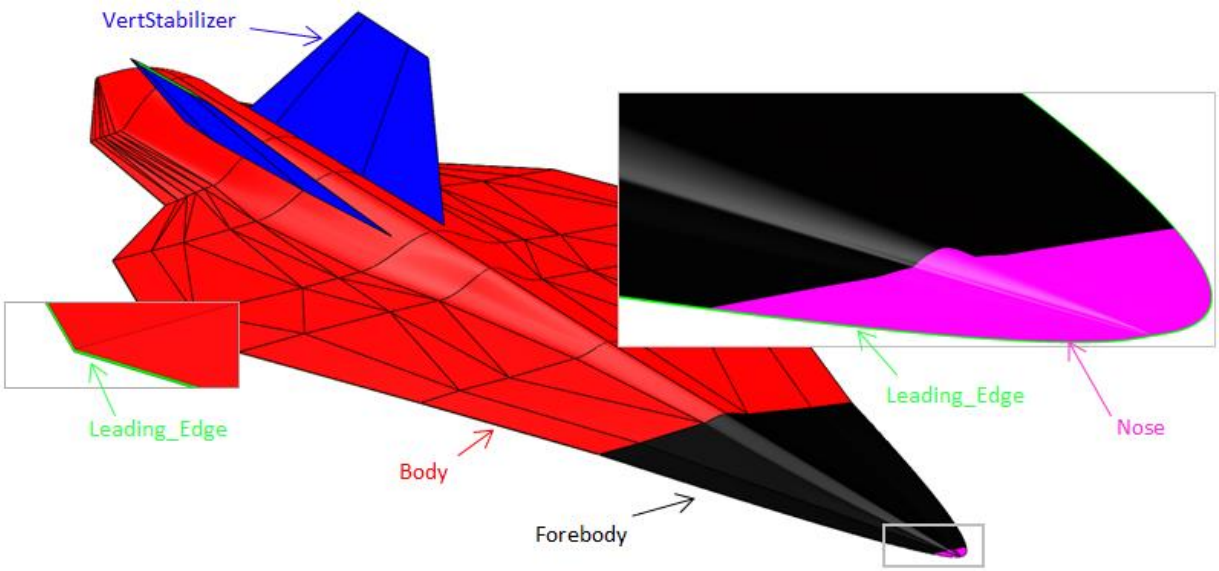

Figure 5.3: Naming conventions from iMod.

All regions in Figure 5.3 are assigned wall boundary conditions. The symmetry and free stream (not shown) are created within STAR-CCM+ and maintain their continua settings from the template. The body (red) region represents the bulk of the geometry and is assigned larger target mesh values. Leading edge (green) regions are located along the body, forebody, nose, and vertical stabilizers. The tips and trailing edges of the stabilizers are also included with green leading edge regions. To comply with best practices, no fewer than two cell thicknesses are permitted along the leading edges and are usually resolved to four cell thicknesses. Vertical stabilizers (blue) cells are proportionately sized relative to the body.

Nose (magenta) and forebody (black) faces are split from the main body to specify finer prism layer control for improved capturing of the thin boundary layer in those locations.

Freestream flow conditions are driven from a table set up using Excel. Triggered by iterations, the table sets the flow parameters throughout the simulation. Among the parameters are: flow direction (XYZ components), Mach number, pressure, and temperature. Table 5.3 is the free stream table used for this study. Unit labels are not included in the actual table headings; however, they are included below for completeness.

Table 5.3: Free stream flow conditions for variation studies.

Iteration	X	Y	Z	Pitch (deg)	Yaw (deg)	Roll (deg)	Mach	P (Pa)	T (°K)
1	-0.9994	0	0.0349	-2	0	0	6	950	228.05
500	-0.9998	0	0.0175	-1	0	0	6	950	228.05
1000	-1.0000	0	-0.0000	0	0	0	6	950	228.05
1500	-0.9998	0	-0.0175	1	0	0	6	950	228.05
2000	-0.9994	0	-0.0349	2	0	0	6	950	228.05
2500	-0.9986	0	-0.0523	3	0	0	6	950	228.05
3000	-0.9976	0	-0.0698	4	0	0	6	950	228.05
3500	-0.9962	0	-0.0872	5	0	0	6	950	228.05
4000	-0.9945	0	-0.1045	6	0	0	6	950	228.05
4500	-0.9925	0	-0.1219	7	0	0	6	950	228.05

Pitch, roll, and yaw columns are indirectly used to generate the components for the X, Y, and Z columns using the Eulerian transformations from Eq. 4.3, Eq. 4.4, and Eq. 4.5. Because the CFD simulation modifies the free stream flow direction and does not rotate the mesh, positive aircraft pitch, roll, and yaw is achieved through negative pitch, roll and yaw transformations of the free stream. The free stream Mach number is equal to 6 and atmospheric pressure and temperature represent a 500 pound per square foot (PSF) dynamic pressure.

5.6 Performance Evaluations

Configuration performance is based on 4 criteria: 1) Lift to drag ratio, 2) Range, 3) Total volume, and 4) Static stability (static margin). All performance metrics are then weighted and combined to provide an overall vehicle performance. The model variations follow a short-hand naming convention of PSx_Vy. Where x represents the phase (design cycle iteration) the model variation corresponds to, in this case PS01 is for phase

#01 and y represents the variation number. PS01_V01 is the first variation and is considered the baseline.

5.6.1 L/D + Breguet Range Equation

Primarily used to compute each variations range capability using the standard Breguet range equation [20] from Section 4.2.1. Separately inspecting the values for aerodynamic performance provides concise correlated feedback from each design modification. Figure 5.4 presents these finding for the first 56 configurations relative to the set target L/D of 6.5.

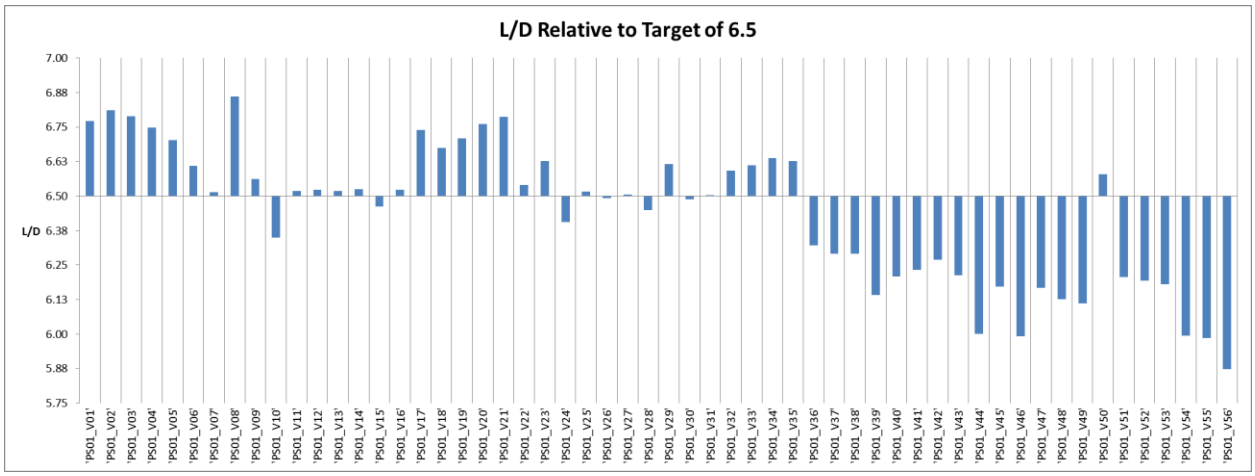

Figure 5.4: Individual lift to drag ratios for 56 variations.

L/D values falling below the target are indicated by negative values below the horizontal axis; values exceeding the target are positive and rise above the horizontal axis.

Figure 5.5 uses L/D values from each variation and represents the performance in terms of the cruise range using the Breguet range equation. The equation assumes a constant TSFC equal to 2.50 $\left(\frac{lb_m/h}{lb_f}\right)$ and velocity of 3589 knots. The L/D values for each variation are also held constant.

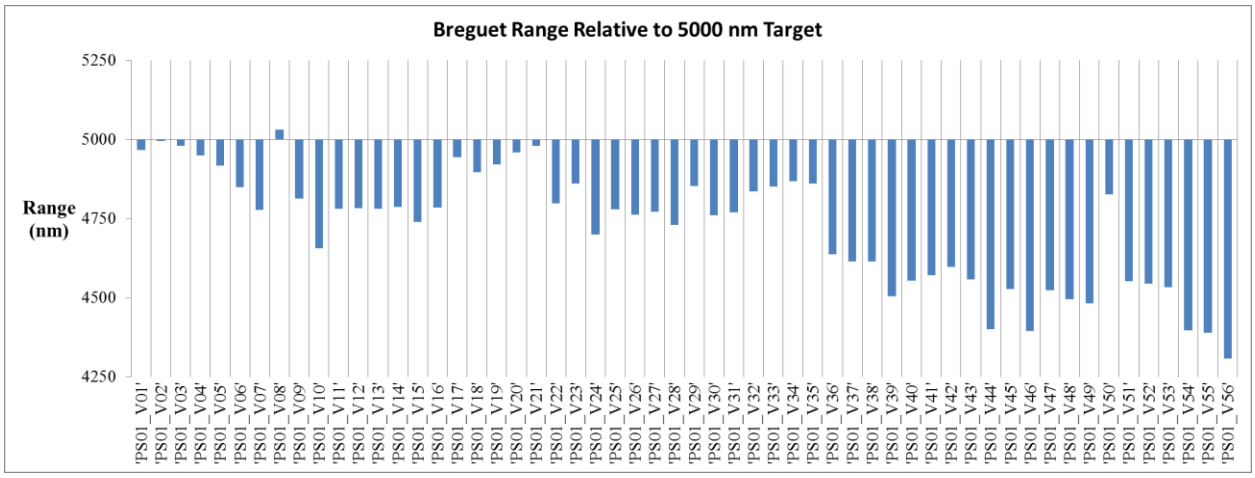

Figure 5.5: Breguet range evaluations relative to 5000 nm target.

The Breguet range analysis above is only applied over the cruise portion of the trajectory, and assumes thrust = drag and lift = weight. This approximation is very optimistic and should be used primarily as a tool for comparison and identifying trends.

5.6.2 Volume + Modified Breguet Range Equation

Similar to the L/D metric, it is also important to monitor the volume as a standalone quantity to identify correlations with design variable changes. A bar graph in Figure 5.6 represents the volume findings for each of the 56 variations as +/- values relative to the baseline configuration.

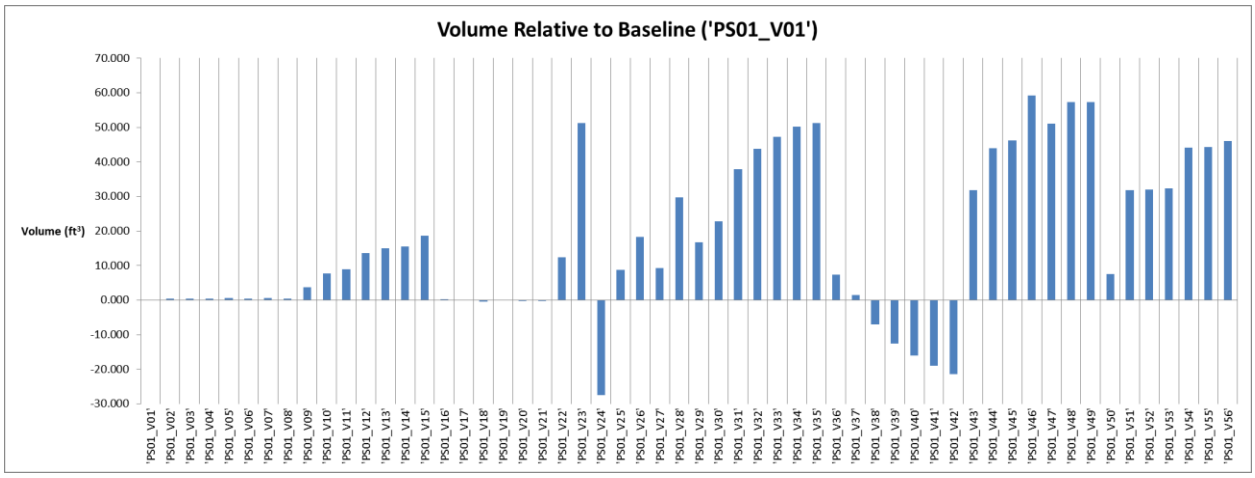

Figure 5.6: Volume breakdowns for each model variation.

Changes in volume are also used to compute a modified form of the Breguet range equation (Eq. 5.1). This modification improves the cruise range comparisons between variations by accounting for the changes in total volume. Larger volumes enable more space for allocating fuel storages and vise-versa. Eq. 5.2 and Eq. 5.3 quantify the approach used in determining the additional term (*Δfuel)* in the Breguet range equation (Eq. 5.1).

$$R = \frac{L}{D}\frac{V}{TSFC} ln\left(\frac{W_i + \Delta fuel}{W_f}\right) \qquad \text{Eq. 5.1}$$

The *Δfuel* term is calculated assuming the 4,000 lb. fuel capacity from the requirements and the total volume of the baseline configuration. Eq. 5.2 is used to calculate the baseline fuel fraction (FF).

$$FF = \frac{W_{fuel}}{V_{baseline}} \qquad \text{Eq. 5.2}$$

Where W_{fuel} is the weight of the fuel (4,000 lb.) and $V_{baseline}$ is the total volume (155.8 ft^3) for the baseline variation. This equates to a fuel fraction of 25.66 pounds/ft^3. The final value for *Δfuel* is calculated for each variation using Eq. 5.3.

$$\Delta fuel = (V_{current} - V_{baseline}) * FF \qquad \text{Eq. 5.3}$$

The result from Eq. 5.3 represents the differences in fuel weight using the volumetric proficiency or deficiency of each variation relative to the baseline. Figure 5.7 shows the modified Breguet cruise range variations relative to the 5000 nm target set by the requirements.

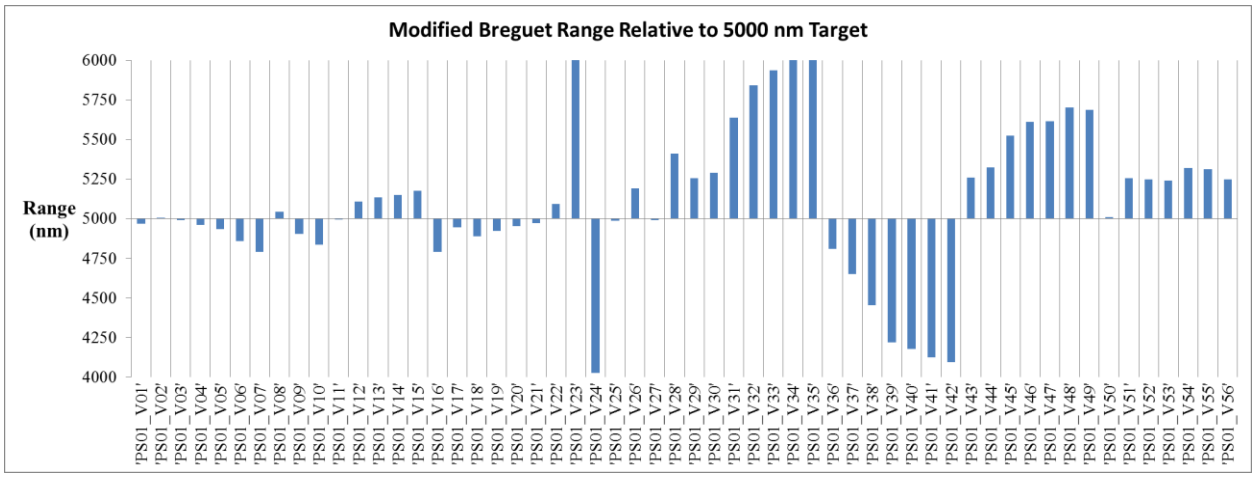

Figure 5.7: Modified Breguet range evaluations for cruise relative to the 5000 nm target.

It can be observed that the results from the modified range equation are significantly improved over the unaltered equation and follow a trend more closely related to the variation volumes than L/D. This is due to relatively minor differences in L/D ratios compared to the fluctuations in fuel capacity.

5.6.3 Range from Energy-State Approximation

The following range findings utilize the methods from Leland M. Nicolai's optimal trajectories for a ramjet propulsion based aircraft [2]. The code used to produce the results was written by Brad Kirkpatrick [21]. Opposed to the previous Breguet range results which assume 100% the fuel is used for cruise, the energy-state approximation assumes ramjet propulsion accelerates the aircraft through the climb phase. The range estimates between the two methods are apparent in the figures that follow. Data required to run the code involves simulating the aircraft of interest at several Mach numbers and altitudes to attain C_L and C_D

results. While assuming a constant thrust to weight ratio, the code runs a minimum fuel consumption (maximum range) trajectory. Aircraft performance is interpolated through the simulated points at defined altitudes to establish a combination of altitude and velocity, thus a dynamic pressure, to maximize energy height gain per unit mass of fuel. Four variations are selected for this analysis; the original baseline (PS01_01), two top contending configurations from the previous Breguet range analysis (PS01_V35 and PS01_V33), and a lower performing variant (PS01_V16) for comparison. Figure 5.8 through Figure 5.11 show the resulting trajectories plots of altitude and range with variations in Mach number. The red scatter points are projections of the trajectory (black) data onto each of the planes to represent the three dimensional data points as 3 separate two dimensional data sets. Plane representations are as follows: lower plane, Range vs. Mach #; right plane, Mach # vs Altitude; and the left plane, Range vs Altitude.

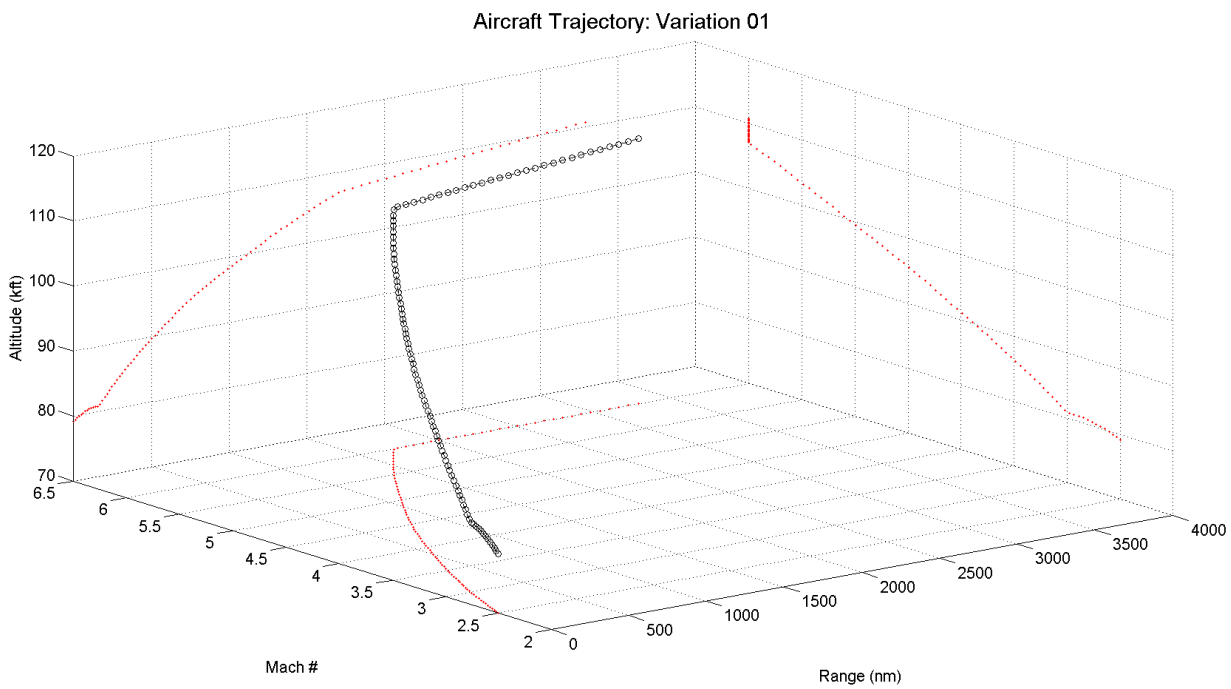

Figure 5.8: Energy method trajectory results: Baseline configuration (PS01_V01).

Energy-state approximations yield an overall range of 3,289 nm in 68 minutes. This method underperforms findings from the unmodified Breguet range analysis by 1677 nm. The aircraft is also estimated to reach its cruise Mach number (M=6) at 1,742 nm down range and an altitude of 107,000 feet. Time to reach this cruise condition is 42 minutes. The next

two figures represent PS01_V35 and PS01_V33. L/D performances of these two aircraft are 6.61 and 6.63, respectively; very close to PS01_V01 with an L/D = 6.77.

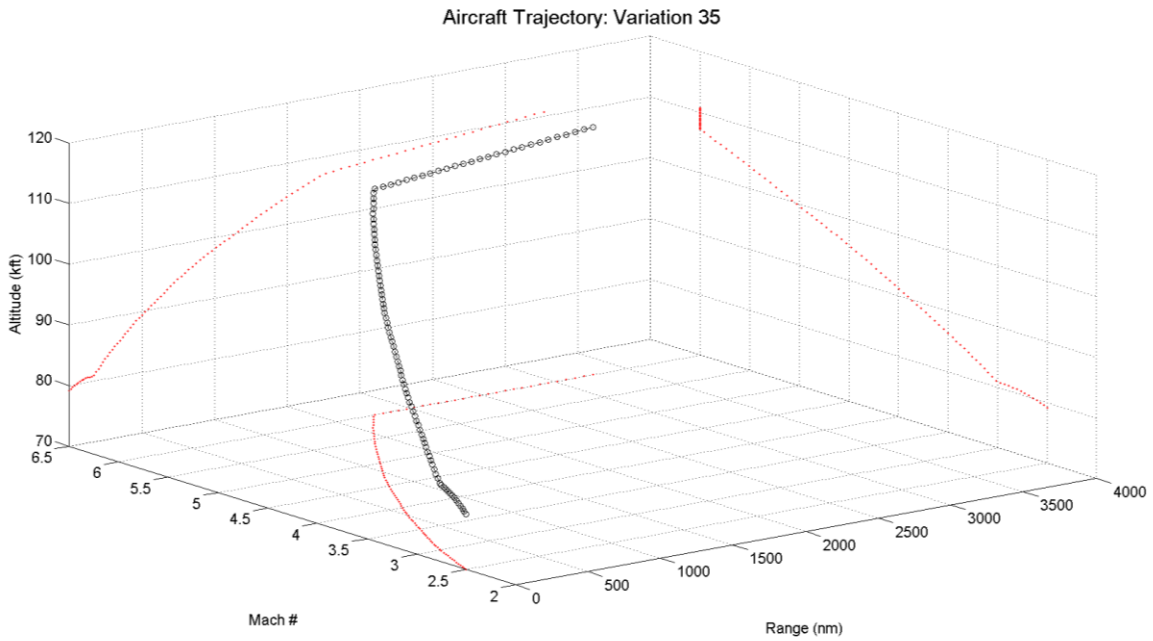

Figure 5.9: Energy method trajectory results: Baseline configuration (PS01_V35).

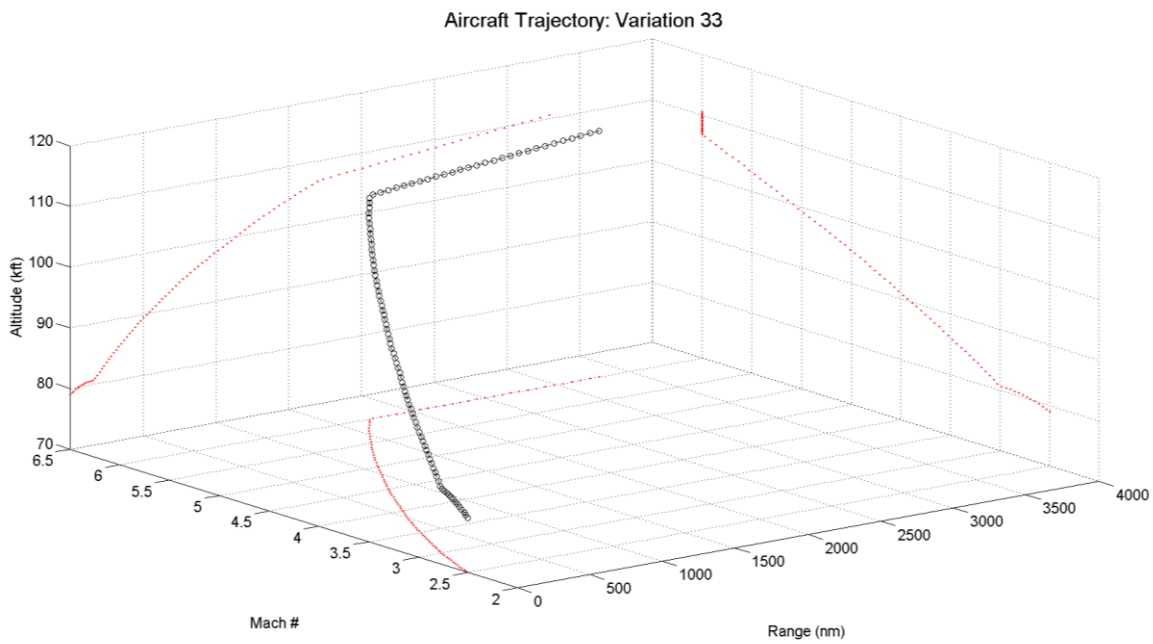

Figure 5.10: Energy method trajectory results: Baseline configuration (PS01_V33).

Compared to the baseline, with an L/D = 6.77, the energy-state trajectories of PS01_V35 and PS01_V33 are very comparable. PS01_V35 has a range of 3,265 nm while PS01_V33 reaches 3,290 nm. PS01_V35 and PS01_V33 both reach their maximum ranges in the same 68 minute time frame as PS01_V01. Similarities for all three configurations extend beyond flight variations of only a few seconds. PS01_V33 reaches an altitude of 110,607 feet. PS01_V35 reaches maximum altitude of 110,807 feet; only 1 foot shy of PS01_V01. Climb data for variations 33 and 35 is also nearly identical to PS01_V01.

Figure 5.11 represents the trajectory of PS01_V16, one of the lowest performing variants from the Breguet range analysis. This configuration is analyzed to demonstrate result sensitivities for the energy-state approximation. Variation 16 has an L/D = 6.52 and a significantly lower reference area (A_{ref} = 273.83 ft^2). For comparison, reference areas for the other three configurations are 338 ft^2 for Variation 01, 334 ft^2 for Variation 33, and 341 ft^2 for Variation 35. A result of the reduced lifting surface area is a dramatic reduction in C_L, and thus, lifting force. This decline drives the aircraft to fly at much higher dynamic pressures in order to accelerate the aircraft to higher altitudes. While the other three previous configurations average dynamic pressures are approximately 375 PSF, Variation 16 does not fall below 400 PSF and averages approximately 550 PSF throughout its flight trajectory.

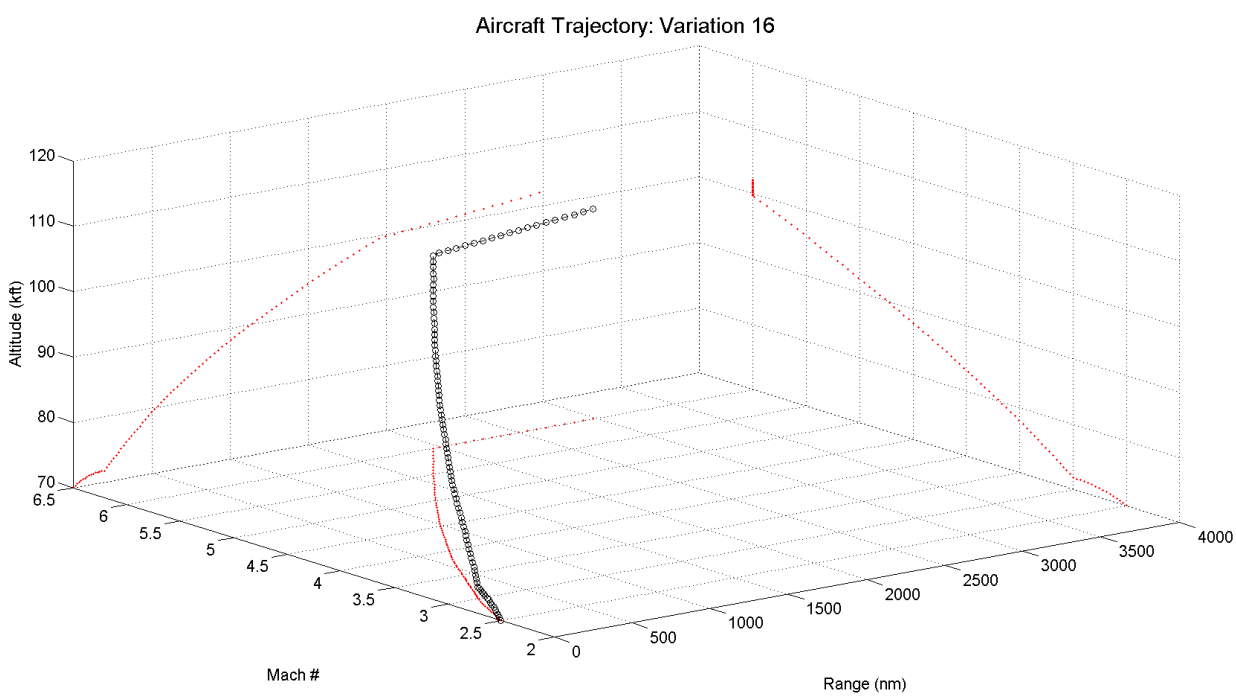

Figure 5.11: Energy method trajectory results: Baseline configuration (PS01_V16).

Results from Figure 5.11 reveal a substantial decrease in range and altitude compared to Variations 01, 33, and 35. The final altitude is 102,086 feet at a range of 2,979 nm. Total flight duration is 65 minutes 45 seconds.

5.6.4 Static Stability

Force and moment data exported from STAR-CCM+ as .csv files is imported into MatLab. The script applies Eulerian rotation transformations to convert the raw data into lift, drag, and pitching moment. The static margin (Eq. 5.6) is calculated using the aerodynamic center (Eq. 5.4) and neutral point (Eq. 5.5). The x-distances for the equations below are measured relative to the nose. For the CFD simulations, this point corresponds to the origin.

$$X_{ac} = \frac{M_{(L/D)_{max}}}{L_{(L/D)_{max}}} \qquad \text{Eq. 5.4}$$

Because the primary point of interest is where the aircraft is at maximum L/D, the aerodynamic center is calculated using lift and moment values that correspond to this condition. For a majority of the variations, maximum L/D occurs at approximately 4° ±1° angle of attack (AoA).

$$\mathrm{X_{np}} = \frac{\partial C_m}{\partial C_L} = \frac{\partial M_y}{\partial L} \qquad \text{Eq. 5.5}$$

The neutral point is the location at which the pitching moment does not change for small changes in AoA. It is also the position where the COG would be placed for a neutrally stable aircraft. The y-axis is the pitching axis, and thus the moment is taken about this direction. The partial derivatives for M_y and L may be simplified into the slope values for each variables linear regression line.

$$\mathrm{SM} = \frac{(X_{ac} - X_{np})}{\bar{c}} * 100 \qquad \text{Eq. 5.6}$$

The variable $\bar{c}$ is the mean aerodynamic chord (MAC) length. Because the overall vehicle length never varied from 10 meters and the span fluctuations were relatively minor in comparison, a constant MAC is designated for all configurations. This value is set at 6.5 meters. For human piloted aircraft a static margin greater than 5% can serve as rough initial estimate for longitudinal stability [18]. The BWB design of this study is not intended to have

a human pilot; however, for the hypersonic speeds at which it travels pitch stability is vital – even with an advanced control system. For this study, a slight reduction in static margin is considered feasible and values assessed above +4.0% are deemed statically stable. The static margin is calculated for each variation relative to the 4% target and displayed in the column chart of Figure 5.12.

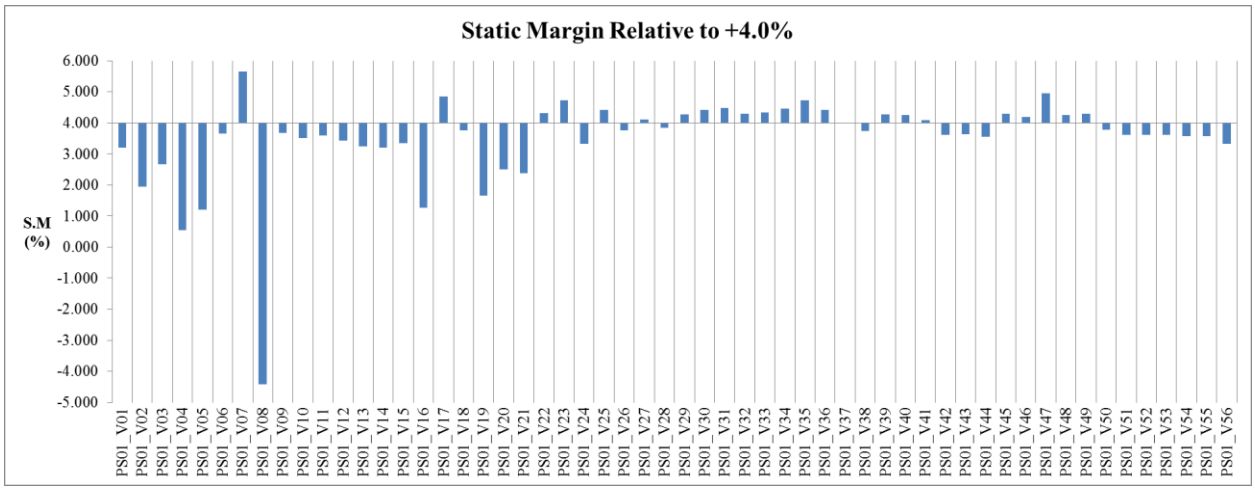

Figure 5.12: Static margin values for each variation (relative to the 4.0% target).

5.6.5 Lift

Lift is selected as a metric to eliminate designs which do not produce enough upward force to overcome the weight of the aircraft during flight. A summary of the lifting values is included in Figure 5.13 relative to the 10,000 pound target. These quantities are the maximum lift values for the aircraft which occur at the maximum simulated AoA of 7°.

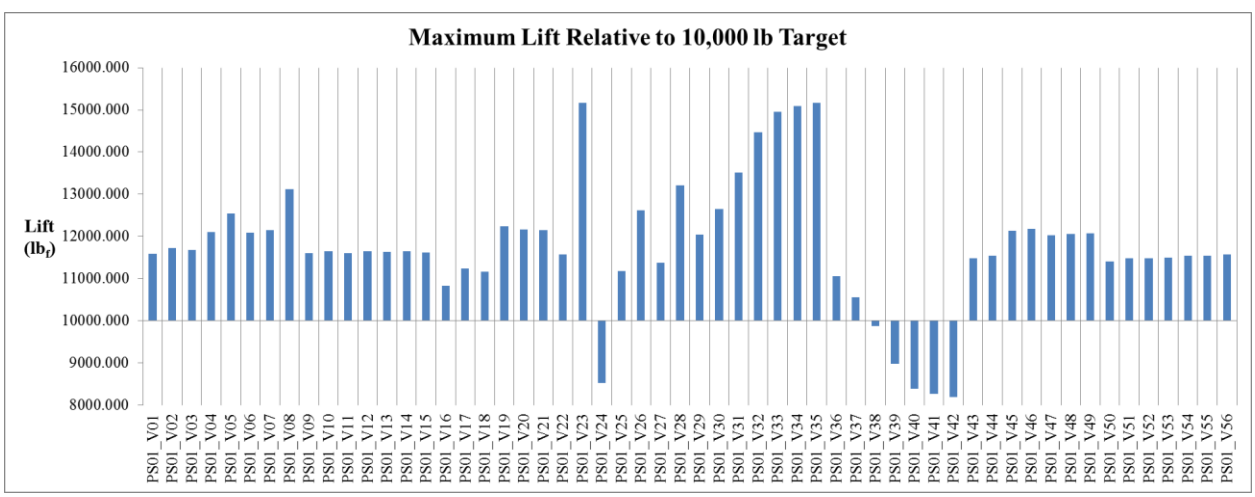

Figure 5.13: Lift relative to 10,000 lb_f target for each variation.

CHAPTER 6. CONCLUSION

The results of this study have proven the value of incorporating robust parametric modeling practices in the conceptual design phase. The time required to complete this full study on a single desktop workstation with 16 processing cores is detailed in Table 6.1.

Table 6.1: Summarized timeline of this study.

Task	Approximate Time Duration
Construct baseline iMod	28 hrs.
Create additional 55 variations	4 hrs.
Simulate 56 variations at 10 angles of attack	1 week
Write MatLab scripts to post process data	16 hrs.
Post processing	8 hrs.
Derive correlations from data	8 hrs.

Total ≈ 232 hrs.

This total time estimate assumes all tasks are completed in consecutive order. However, this is only true for the first three tasks. If the MatLab scripts are written while the simulations run and 8 hour work days are used, the total time for completion is 13 days assuming the simulations run 24 hours/day. The total billable engineering hours only totals 64, as there is no human interaction with the simulation processes. This time table is only applicable for the first iteration through the conceptual design cycle. All additional cycles will not require the build time for the first conceptual baseline iMod or the time to write the MatLab post processing scripts. If MatLab post processing scripts are written to organize and plot data in a meaningful manner, the time to derive correlations may also be drastically reduced. The most significant gains for the simulation based design process will come from computational resources. If simulation time can be reduced to match the time required to post process and derive meaningful correlations from the data, future cycle time can be reduced to a meager two days or less. This can be achieved with an additional 56 processing cores; just slightly over 3 identical workstations.

By using the top down approach, each design team has the ability to filter features of the iMod which do not pertain to their current analysis. Parent-child relations enable engineers to track these changes and monitor their effects on other design parameters. The BWB iMod constructed in section 3.4 proves the capability of solid modeling and establishes

the superiority it has over surface modeling. It should be noted that the process of developing iMods is not an exact science and special care must be taken when creating parametric relations. In practice, this requires acute attention to detail coupled with strict guidance from expert design engineers to capture complete aircraft functionality. iMod development constantly evolves during the design phases to enhance current constructs and reconcile newly discovered design defects. This is a learning process for both the engineers developing the iMod and the veteran engineers guiding them along the way.

6.1 Future Work

Introducing the full spectrum of design disciplines into the conceptual phase will provide engineers with a more comprehensive analysis. Additional CAE tools which allow seamless integration into a simulation based design process includes structural finite element analysis. Abaqus has been used in conjunction with STAR-CCM+ to map pressure contours from the finite volume CFD mesh to the finite element FEA mesh. By having a structural design team capable of constructing internal structures, regions susceptible to failure can be identified and corrected early. Propulsion integration is another critical system component to the conceptual design phase. Without engine sizing data, the aerodynamics team is left to make gross and uninformed approximations for inlet capture area and nozzle exit area. Propulsion system integration will also provide more accurate results for installation penalties as they relate to aerodynamic performance. Total volume estimates, subsystem placements for COG location, and additional reinforcement structures are other among other design considerations highly dependent on propulsion integration. When aforementioned systems are integrated into the conceptual design phase, a model with detailed mass properties can provide mass moments of inertia for dynamic stability analysis. STAR-CCM+ is capable of computing transient flow simulations using 6 degrees of freedom (DOF) to compute dynamic performance. Each of these systems along with their subsystems and components require substantially increasing the level of detail for the parametric iMod.

BIBLIOGRAPHY

[1] P. W. G. Morris and J. Geraldi, "Managing the Institutional Context for Projects," *Project Management Journal,* vol. 42, no. 6, pp. 20-32, 2011.

[2] L. M. Nicolai, Fundamental of Aircraft and Airship Design, Reston, Virginia: American Institute of Aeronautics and Astronautics, 2010.

[3] P. PERRIER, "Computational Procedures for Preliminary Design," in *Special Course on Engineering Methods in Aerodynamic Analysis and Design of Aircraft*, Neuilly Sur Seine, France, AGUARD, 1992, pp. 2-4.

[4] F. A. Salustri, "An Extremely Abbreviated History of Engineering Design," Department of Mechanical and Industrial Engineering, Ryerson University, 27 12 2005. [Online]. Available: http://deed.ryerson.ca/~fil/t/history0.html. [Accessed 16 07 2014].

[5] T. P. Gielda, B. Webster, c. Hutton and R. Sandboge, "Simulation Based Design," in *Daratech IPDS*, Novi, MI, 2001.

[6] T. P. Gielda, "Past, Present and future Role of CAE in Auomotive Thermal Management," in *VTMS Conference*, Nashville, TN, 2001.

[7] T. P. Gielda, "Simulation Based Design in the Appliance Industry," in *ASME Fluids Engineering Conference*, Charlotte, NC, 2004.

[8] P. T. Harsha, L. C. Keel, R. T. Sherill and A. Castrogiovanni, "X-43A Vehicle Design and Manufacture," *AIAA/CIRA*, vol. 13th International Space Planes and Hypersonics Systems and Technologies, no. May, 2005.

[9] J. C. Goodall and N. D. Goodall, Black Jets, Norwalk, CT: AIRime, 1999.

[10] K. G. Bowcutt, "Multidisciplinary Optimization of Airbreathing," *Journal of Propulsion and Power,* vol. 17, no. 6, pp. 1184-1190, 2001.

[11] K. G. Bowcutt, "Hypersonic Vehicle System Integration," in *Hypersonic Educational Initiative*, Hampton, Virginia, 2007.

[12] M. K. Smart, "Design of three-dimensional hypersonic inlets with rectangular-to-elliptical shape transition," *Journal of Propulsion and Power,* vol. 15, no. 3, pp. 408-416, 1999.

[13] STAR-CCM+, Transonic/Supersonic External Aerodynamics: Steady State RANS Approach, 8.06.005 ed., Melville, NY: CD-adapco, 2014.

[14] M.-S. Liou, "A Sequal to AUSM: AUSM+," *Journal of Computational Physics,* vol. 129, no. 1, pp. 364-382, 1996.

[15] F. R. Menter, "Two-Equation Eddy-Viscosity Turbulence Models for Engineering Applications," *AIAA,* vol. 32, no. 8, pp. 1598-1605, 1994.

[16] D. E. Glass, "Leading Edges," in *National Institude of Aerospace - Hypersonic Educational Initiative*, Hampton, Virginia, 2007.

[17] L. V. Schmidt, Introduction to Aircraft Flight Dynamics, Reston, Virginia: AIAA, 1998.

[18] W. F. Phillips, Mechanics of Flight, Second Edition ed., Hoboken, New Jersey: John Wiley & Sons, 2010, pp. 400-409.

[19] T. D. Blackburn, T. A. Mazzuchi and S. Sarkani, "Using a TRIZ Framework for Sysems Engineering Trade Studies," *Systems Engineering,* vol. 15, no. 3, pp. 355-367, 2012.

[20] D. P. Raymer, Aircraft Design: A Conceptual Approach, Fourth ed., Reston, Virginia: American Institute of Aeronautics and Astronautics, 2006.

[21] B. K. Kirkpatrick, *Propulsion integration of hypersonic air-breathing vehicles utilizing a top-down design methodology,* Ames, IA: Iowa State University, 2014.

[22] D. R. Jenkins, Lockheed SR-71/YF-12 Blackbirds, vol. 10, North Branch, MN: Specialty Press, 1997.

[23] M. Williamson, "Hypersonic Transport," *Aerospace America,* pp. 40-45, May 2012.

[24] U.S. Department of Defense, "Acquisition of Major Defense Systems: DoD Directive 5000.1," Government Printing Office, Washington, D.C., 2009.